










GDNF gene therapy for alcohol use disorder in male non-human primates

Received: 12 October 2022

Accepted: 15 June 2023

Published online: 14 August 2023


 Check for updates

Matthew M. Ford ^{1,2,6}, Brianna E. George ^{3,6}, Victor S. Van Laar ^{4,6}, Katherine M. Holleran^{3,6}, Jerusha Naidoo^{4,5}, Piotr Hadaczek^{4,5}, Lauren E. Vanderhooft¹, Emily G. Peck ³, Monica H. Dawes ³, Kousaku Ohno⁵, John Bringas⁵, Jodi L. McBride¹, Lluís Samaranch^{4,5}, John R. Forsayeth⁵, Sara R. Jones³, Kathleen A. Grant ¹  & Krystof S. Bankiewicz ^{4,5} 

Alcohol use disorder (AUD) exacts enormous personal, social and economic costs globally. Return to alcohol use in treatment-seeking patients with AUD is common, engendered by a cycle of repeated abstinence-relapse episodes even with use of currently available pharmacotherapies. Repeated ethanol use induces dopaminergic signaling neuroadaptations in ventral tegmental area (VTA) neurons of the mesolimbic reward pathway, and sustained dysfunction of reward circuitry is associated with return to drinking behavior. We tested this hypothesis by infusing adeno-associated virus serotype 2 vector encoding human glial-derived neurotrophic factor (AAV2-hGDNF), a growth factor that enhances dopaminergic neuron function, into the VTA of four male rhesus monkeys, with another four receiving vehicle, following induction of chronic alcohol drinking. GDNF expression ablated the return to alcohol drinking behavior over a 12-month period of repeated abstinence–alcohol reintroduction challenges. This behavioral change was accompanied by neurophysiological modulations to dopamine signaling in the nucleus accumbens that countered the hypodopaminergic signaling state associated with chronic alcohol use, indicative of a therapeutic modulation of limbic circuits countering the effects of alcohol. These preclinical findings suggest gene therapy targeting relapse prevention may be a potential therapeutic strategy for AUD.

Recent epidemiological studies on alcohol consumption estimate an annual cost of \$249 billion on the US economy associated with alcohol use, with 140,000 deaths per year in the United States attributed to alcohol use disorder (AUD) and an estimated 12% of all alcohol consumers meeting the criteria for AUD as defined by the *Diagnostic and Statistical Manual for Mental Disorders* fifth edition^{1–3}. Despite these numbers, few

US Food and Drug Administration-approved pharmacotherapies are currently available, and continued medication adherence is noted as the most significant obstacle to positive treatment outcomes^{4,5}. Therapeutic approaches that directly target the underlying brain circuitry adaptations concurrent with sustained heavy drinking are missing and would add a new dimension to available treatments for patients with AUD.

¹Division of Neuroscience, Oregon National Primate Research Center, Oregon Health & Science University, Portland, OR, USA. ²Department of Psychology, Lewis & Clark College, Portland, OR, USA. ³Department of Physiology and Pharmacology, Wake Forest School of Medicine, Winston Salem, NC, USA. ⁴Department of Neurological Surgery, The Ohio State University, Columbus, OH, USA. ⁵Department of Neurological Surgery, University of California, San Francisco, CA, USA. ⁶These authors contributed equally: Matthew M. Ford, Brianna E. George, Victor S. Van Laar, Katherine M. Holleran.  e-mail: grantka@ohsu.edu; Krzysztof.Bankiewicz@osumc.edu

Neuroadaptation in brain network mediating motivated behavior occurs as a consequence of chronic, intermittent alcohol exposure⁶. These alterations are thought to underlie the preoccupation with drinking alcohol in AUD, despite social or interpersonal problems⁶. The most pronounced neurological deficit in development of AUD is in mesolimbic dopamine (DA) signaling^{6–8}. Individuals diagnosed with severe AUD, as well as rodents and non-human primates (NHPs) in models of AUD, present with impaired DA release mechanisms within mesolimbic projections from the ventral tegmental area (VTA) to the nucleus accumbens (NAc), including reduced levels of DA, altered DA autoreceptor sensitivity and increased rates of DA reuptake at dopaminergic (DAergic) terminals, resulting in a ‘hypodopaminergic’ state^{9–12}. Further, rodent models of AUD have abundantly demonstrated that DA signaling regulates alcohol self-administration^{13–16}.

Glial-derived neurotrophic factor (GDNF) protein influences accumbal DA signaling and alcohol use through its integral role in the function of DAergic neurons^{14,17}. Acute alcohol exposure elicited an upregulation of GDNF expression in the mesolimbic system, whereas chronic intermittent alcohol use led to decreased endogenous GDNF expression in rodents and reduced GDNF serum levels in patients with AUD during abstinence^{18,19}. Correspondingly, GDNF knockdown in the VTA escalated the onset of alcohol self-administration in rodents^{15,18}, whereas increasing GDNF in the VTA attenuated alcohol-seeking and self-administration behaviors^{16,20–23}. Collectively, these findings indicate that GDNF is a critical modulator of the mesolimbic DA signaling system and has the potential to normalize alcohol intake in individuals with AUD²⁴.

We describe a gene therapy approach to address AUD, offering the advantage of a one-time, sustained disease-modifying treatment. We examined the utility and efficacy of delivering AAV2 vector into the VTA to induce constitutive expression of GDNF, ablate alcohol use and prevent post-abstinence resumption of drinking using a rhesus macaque model of AUD. We posited that the sustained GDNF expression in the VTA will selectively prevent excessive drinking following abstinence while not disrupting other motivated behaviors. This treatment approach, targeting chronic alcohol-induced deficits in mesolimbic DAergic function, has the potential to circumvent the reliance on protracted patient treatment adherence by preventing relapse.

Results

NHP model recapitulates behaviors of chronic alcohol use

Inability to maintain abstinence and inability to reduce hazardous patterns of drinking are two main challenges in the treatment of patients with AUD. To model this behavior, an established protocol for the induction and maintenance of alcohol consumption in male macaque monkeys was employed that incorporates multiple cycles of daily intoxication followed by abstinence from alcohol, as described in patients with AUD (Fig. 1a)^{25–27}. Alcohol was introduced by using escalating doses of daily ethanol self-administration followed by a 6-month open access baseline (OAB) period during which subjects had access to both water and an ethanol solution (4% w/v) for 22 h per day. Pairwise comparisons revealed mean daily alcohol intakes increased throughout the OAB (Fig. 1b) ($F_{4,80, 33,11} = 2.62, P \leq 0.05$). The average alcohol intake over the 6-month OAB was $2.27 \pm 0.28 \text{ g kg}^{-1}$ per day and held steady at $2.49 \pm 0.09 \text{ g kg}^{-1}$ per day during the final week of OAB (Fig. 1c), the equivalent of approximately 9 drinks per day for an average person²⁵. The alcohol intakes (grams per kilogram) that corresponded with the time of blood sampling were significantly correlated with blood ethanol concentration (BEC) collected throughout the OAB (Fig. 1d; $r = 0.941, P \leq 0.0001$), demonstrating the physiological relevance of consumption patterns. During the last week of the OAB, not only was this correlation maintained, but also BECs approaching or exceeding the NIAAA-defined threshold of $\geq 80 \text{ mg dl}^{-1}$ (0.08%) for binge drinking were documented in six of the eight macaques (Extended Data Fig. 1a)²⁸. During the final week of the OAB, the amount of alcohol consumed by each subject

was stable, with intersubject differences (Fig. 1c,e). Future treatment groups were determined from this data, counterbalancing by the overall mean alcohol intakes during the final week of OAB. The grand means for the future vehicle- and GDNF-treated groups were 2.47 ± 0.28 and 2.51 ± 0.49 , respectively (dashed horizontal lines in Fig. 1e), and did not significantly differ, nor did the positive correlations between BEC and alcohol intake for the two groups (Extended Data Fig. 1b).

AAV2-hGDNF lowers subsequent alcohol intake

At the conclusion of the OAB period, ethanol was replaced with water (that is, forced alcohol abstinence) for 4 weeks before surgical infusion of the therapeutic (Fig. 2). Each monkey was bilaterally infused with either an adeno-associated virus serotype 2 vector encoding human GDNF (AAV2-hGDNF; $2.0 \times 10^{13} \text{ vg ml}^{-1}$ final titer, for example $1.2 \times 10^{12} \text{ vg}$ in the total 60 μl infused per monkey) or vehicle spiked with gadolinium into the VTA via imaging-guided convection-enhanced delivery (MR-guided CED) (Fig. 2)²⁹. The viral titer selected is comparable to doses of AAV2 vector previously found to be safe and tolerable with intra-VTA delivery in NHPs³⁰ and mesolimbic system infusion in rats^{24,31}. In both pilot (Extended Data Fig. 2) and experimental surgeries, no adverse events or vasculature leakage occurred during the infusions (Fig. 2).

Abstinence conditions continued for 2 months after the viral infusion to allow for optimal viral transduction and protein expression (phase A1; Fig. 1a), at which time alcohol access was reintroduced for 4 weeks (phase R1, Fig. 1a). A total of six forced-abstinence/alcohol-reintroduction phases were repeated to model abstinence/resumption of drinking cycles observed from patients with AUD (Fig. 1a). AAV2-hGDNF significantly blunted alcohol intakes during the alcohol reintroduction periods across multiple abstinence/alcohol-reintroduction cycles ($F_{6,36} = 5.00, P \leq 0.001$; Fig. 3a,b). BEC was also reduced to undetectable levels in AAV2-hGDNF-treated subjects throughout R1 and remained undetectable within the group for most weeks in phases R2–R6 (Fig. 3c,d). By contrast, vehicle-treated subjects showed consistently elevated monthly and weekly levels for alcohol intakes and BEC across cycles both as a group (Fig. 3a–d) and individually (Extended Data Fig. 3a,b) and did not differ from their OAB intakes.

Previous work suggested that alcohol drinking transiently increases after periods of abstinence in macaques and patients with AUD^{26,32}. The first post-abstinence day of ethanol availability was therefore separately assessed to evaluate hazardous drinking patterns. Vehicle-treated subjects continued to recapitulate their OAB-period alcohol-drinking routines at each alcohol-reintroduction onset (Fig. 3e,f and Extended Data Fig. 3c), corresponding with a heightened BEC on the first day of onset (Fig. 3d; first data point shown in each R phase). Vehicle-treated subjects also exhibited exaggerated maximum bout sizes in the first session post-abstinence (that is, R5 and R6; $F_{6,36} = 3.39, P \leq 0.01$; Fig. 3f and Extended Data Fig. 3c), demonstrating these subjects were ‘overshooting’ previous average intakes during early alcohol reintroduction, consistent with previous findings²⁶. Conversely, AAV2-hGDNF-treated subjects exhibited a delay to their maximum alcohol-intake bout on the first day post-abstinence in phases R2–R6 as compared to baseline ($F_{1,6} = 82, P \leq 0.0001$) and vehicle-treated subjects ($F_{6,36} = 3.4, P \leq 0.01$) (Fig. 3e and Extended Data Fig. 3c), as well as a significantly decreased amount of alcohol intake at their maximum bout in phases R1–R6 ($F_{1,6} = 18.11, P \leq 0.01$; Fig. 3f and Extended Data Fig. 3c). AAV2-hGDNF-treated subjects also showed a longer delay to first alcohol-intake bout ($F_{1,6} = 12.05, P \leq 0.01$), smaller first bout size ($F_{1,6} = 29.95, P \leq 0.01$) and lower overall grams per kilogram alcohol consumed in the first session post-abstinence ($F_{6,36} = 2.48, P \leq 0.05$) (Extended Data Fig. 3c). Thus, drinking patterns toward alcohol were significantly reduced but not eliminated, suggesting that AAV2-hGDNF treatment did not induce a conditioned taste aversion. Rather, treatment produced a new, durable titration to a reduced level of alcohol intake.

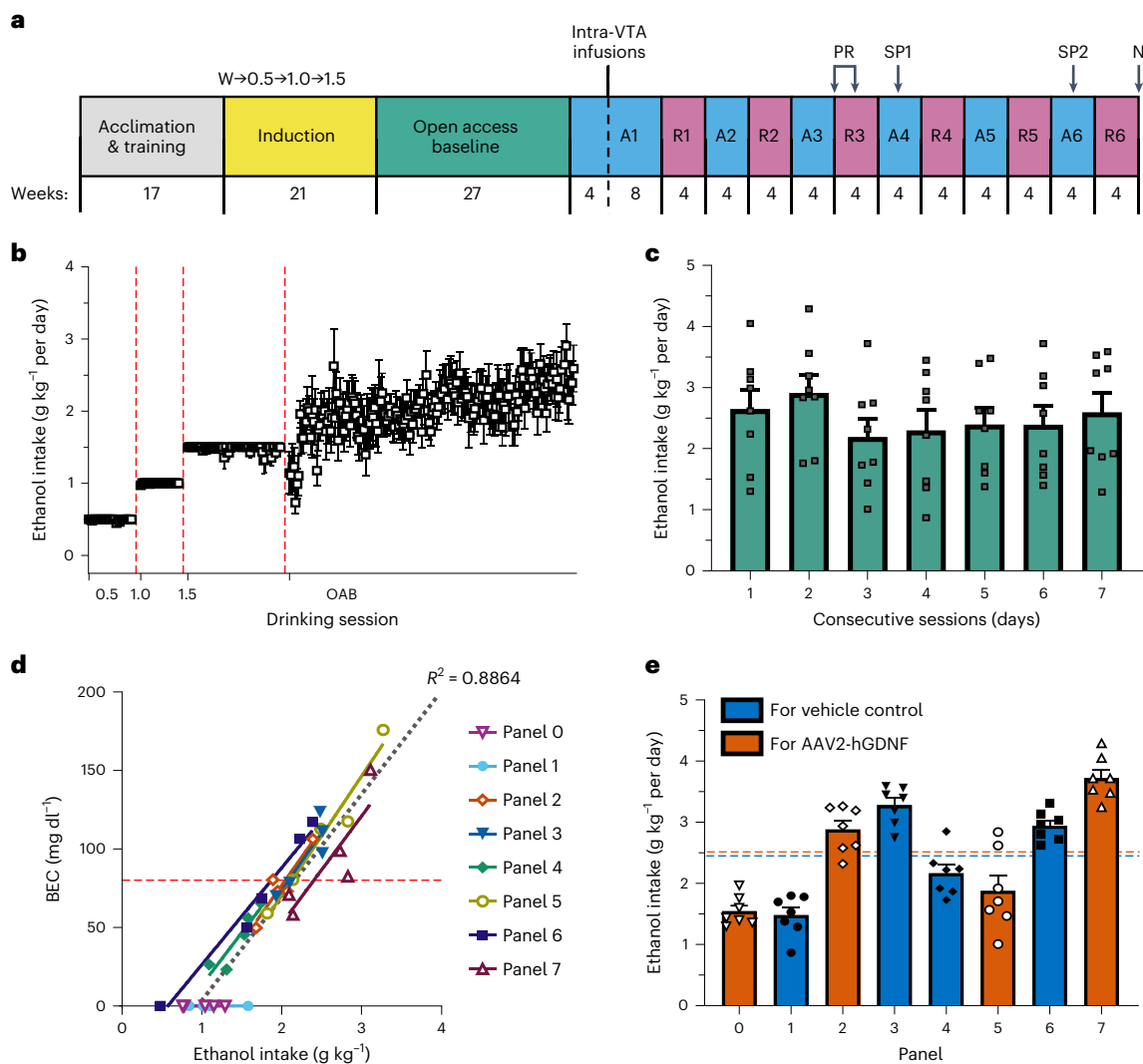


Fig. 1 | Chronic alcohol self-administration in rhesus macaques recapitulates drinking in humans. **a**, Experimental time course design, including 4-month acclimation period, 5-month induction period, 6-month OAB and six 1-month abstinence periods (A1–A6) interspersed by 1-month alcohol reintroduction periods (R1–R6). The number of days in each phase is expressed in brackets. Intra-VTA infusions were performed 1 month into phase A1, followed by two additional months in phase A1 for post-surgical recovery. During the first half of phase R3, the alcohol spout location was reversed ('R') and then reset for the second half to evaluate side bias. Two sucralose probe ('SP') tests were conducted 2 weeks into phases A4 and A6. Necropsy ('N') was performed at the conclusion of phase R6. **b**, The mean alcohol intake (grams per kilogram per day) for male rhesus macaques throughout a four-step induction procedure (water→0.5 g kg⁻¹→1.0 g kg⁻¹→1.5 g kg⁻¹) illustrates an incremental ramping of set dose exposures followed by the onset of daily open free-choice alcohol access (group mean values ± standard error of the mean (s.e.m.), *n* = 8). **c**, Average daily ethanol intake (grams per kilogram per day) for all subjects over the final 7 days of the OAB, demonstrating all subjects readily

drinking alcohol (group mean ± s.e.m., with squares representing individuals, *n* = 8). **d**, The relationship between BECs collected during the final 2 months of the OAB (*n* = 5 BEC measurements per subject) and corresponding alcohol intakes recorded at timing of sampling for each subject as identified by drinking panel each was assigned (panels 0–7), with the dashed horizontal line demarcating 80 mg dl⁻¹ (the threshold for legal intoxication in humans). Linear regression analysis of the grouped BEC data points (*n* = 40) showed a positive linear relationship between EtOH intake and BEC ($R^2 = 0.8864$). **e**, The stability of alcohol intake within individual subjects (panels 0–7) over the final 7 days of the OAB. Subjects destined for future assignment to vehicle or GDNF treatment groups are depicted as blue- or orange-shaded bars, respectively. The mean ± s.e.m. (*n* = 7 days) for each subject is shown. The grand mean for each treatment group is presented by dashed horizontal lines (blue, vehicle; orange, AAV2-hGDNF). Treatment group means for alcohol intake were not significantly different.

Tolerance of AAV2-hGDNF treatment

Food intake. Both treatment groups exhibited a sharp, transitory decline in food-maintenance behavior immediately post-surgery (day 0) that returned to baseline by post-surgical week 1 (Fig. 4a). Vehicle-treated subjects maintained stable baseline levels of food responding thereafter. As a group, GDNF-treated subjects also maintained lower food intake between post-surgical days 11 and 18. This response was transient, returning to baseline between post-surgical weeks 3–6 (Fig. 3a).

Body weight. Vehicle-treated monkeys lost an average of 8% body weight between post-surgical weeks 2–8 (end of phase A1), then slowly resumed weight gain (Fig. 4b). AAV2-hGDNF-treated subjects exhibited a transient weight loss between post-surgical weeks 2–16, with maximal loss averaging 18% from OAB at the end of phase A2 (Fig. 4b and Extended Data Fig. 4a), with a gradual return towards baseline thereafter. AAV2-hGDNF subjects remained 13% below their group baseline weight and vehicle group weight by phase R6 (Fig. 4b). Examination of body condition by a veterinarian during phase A2

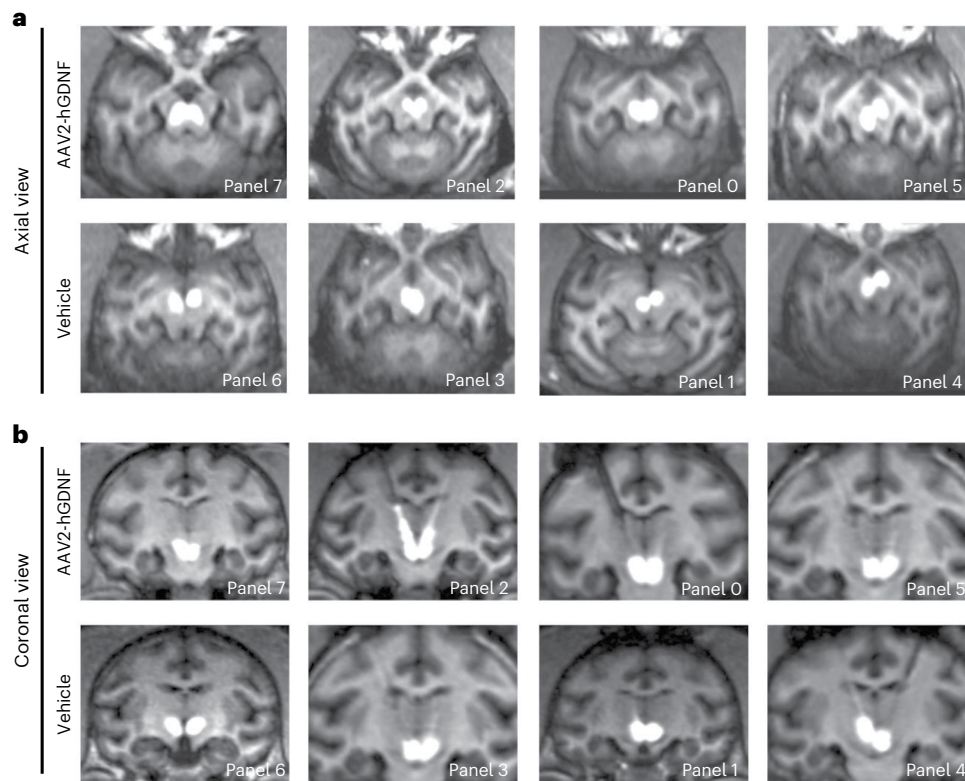


Fig. 2 | AAV2-hGDNF delivery to the VTA. a, b. Representative axial (a) and coronal (b) magnetic resonance (MR) images of bilateral gadoteridol distribution in each GDNF-treated (respective top rows) or vehicle-treated (respective bottom rows) subject following convection-enhanced delivery, indicating successful targeting of the VTA.

determined that all study subjects maintained a score between 2.0 and 3.0 (5-point scale with 1.0 being emaciated, 3.0 being optimal, and 5.0 being obese), and within 0.5 points from their baseline weights³³. GDNF-treated subjects were therefore lean, but within a healthy weight range throughout the study.

Considering the persistent weight difference between groups, we assessed the caloric intake derived from ethanol, an energy-dense source providing 7 kcal g⁻¹. GDNF subjects (0.7–1.1 kcal kg⁻¹ per day) were taking in significantly less ethanol-derived calories daily during R phases as compared to the vehicle-treated group (13.2–15.9 kcal kg⁻¹ per day) ($F_{6,30} = 9.40, P \leq 0.01$; Extended Data Fig. 4c). Accordingly, the rate of weight gain between A3 and R6 was slightly lower in the AAV2-hGDNF group (0.082 kg per month) compared to the vehicle group (0.10 kg per month) (Extended Data Fig. 4d).

Water intake. After surgery, water and total fluid intake volumes of the GDNF-treated group decreased slightly from OAB and were lower than the vehicle-treated group (Fig. 4c,d and Extended Data Fig. 4b), but they were within range of reported daily water intake reported for macaques in other studies^{34,35}. In contrast, water and total fluid intakes increased in vehicle subjects by 67–88% from baseline during abstinence phases (Fig. 4c,d). These observations are in line with a previous study showing higher fluid intake in alcohol-consuming NHPs as compared to naïve controls¹⁰.

Sensorimotor and motivational behaviors. A reach task (reaching for a raisin presented outside the cage) was performed at 1- to 2-week intervals through the peri-surgical period to assess sensorimotor function in three stages, the time to reach for the raisin (stage 1, Fig. 4e), time to grasp the raisin (stage 2, Fig. 4f) and time to return the raisin to their mouth (stage 3, Fig. 4g). The three stages were assessed individually and summed together to assess total time to complete the task (Fig. 4h).

There were intersubject differences in time to reach for the raisin in the first 7 weeks post AAV2-hGDNF infusion; however, these did not reach significance from control (Fig. 4). All subjects normalized to baseline by week 8.

Sucralose was used as a probe for motivated behavior during phases A4 and A6 to examine the impact of GDNF treatment on an alternate reward³⁶. Similar results were obtained between the two independent tests, with GDNF-treated subjects consuming 20% of the available cherry-flavored sucralose solution during six consecutive 1 h presentations, whereas vehicle-treated subjects consumed 100% (Fig. 4i,j).

GDNF protein is increased in mesolimbic regions

Immunohistochemistry revealed increased GDNF protein in the VTA of AAV2-hGDNF brains as compared to vehicle-treated controls, as well as areas of projection including the NAc, ventral putamen and caudate nucleus, resulting from GDNF secretion from VTA axons (Fig. 4a). Using enzyme-linked immunosorbent assay (ELISA) protein quantification, GDNF levels in NAc, ventral putamen and caudate nucleus regions of AAV2-transduced brains were significantly increased as compared to vehicle ($[t_{(df_6)} = 3.8, P \leq 0.01]$, $[t_{(df_6)} = 3.2, P \leq 0.05]$, $[t_{(df_6)} = 2.9, P \leq 0.05]$, respectively; Fig. 5b and Extended Data Fig. 5c). Prefrontal cortex and cingulate gyrus GDNF concentrations were only slightly, but significantly, elevated in GDNF subjects as compared to vehicle ($[t_{(df_6)} = 5.4, P \leq 0.05]$, $[t_{(df_6)} = 6.6, P \leq 0.01]$, respectively; Fig. 5b and Extended Data Fig. 5c). This finding suggests limited GDNF axonal transport via mesocortical pathways as compared to mesolimbic pathways.

AAV2-hGDNF is associated with increased DA levels and turnover

High-performance liquid chromatography (HPLC) detection demonstrated that DA concentrations were 5.8-fold higher in the VTA

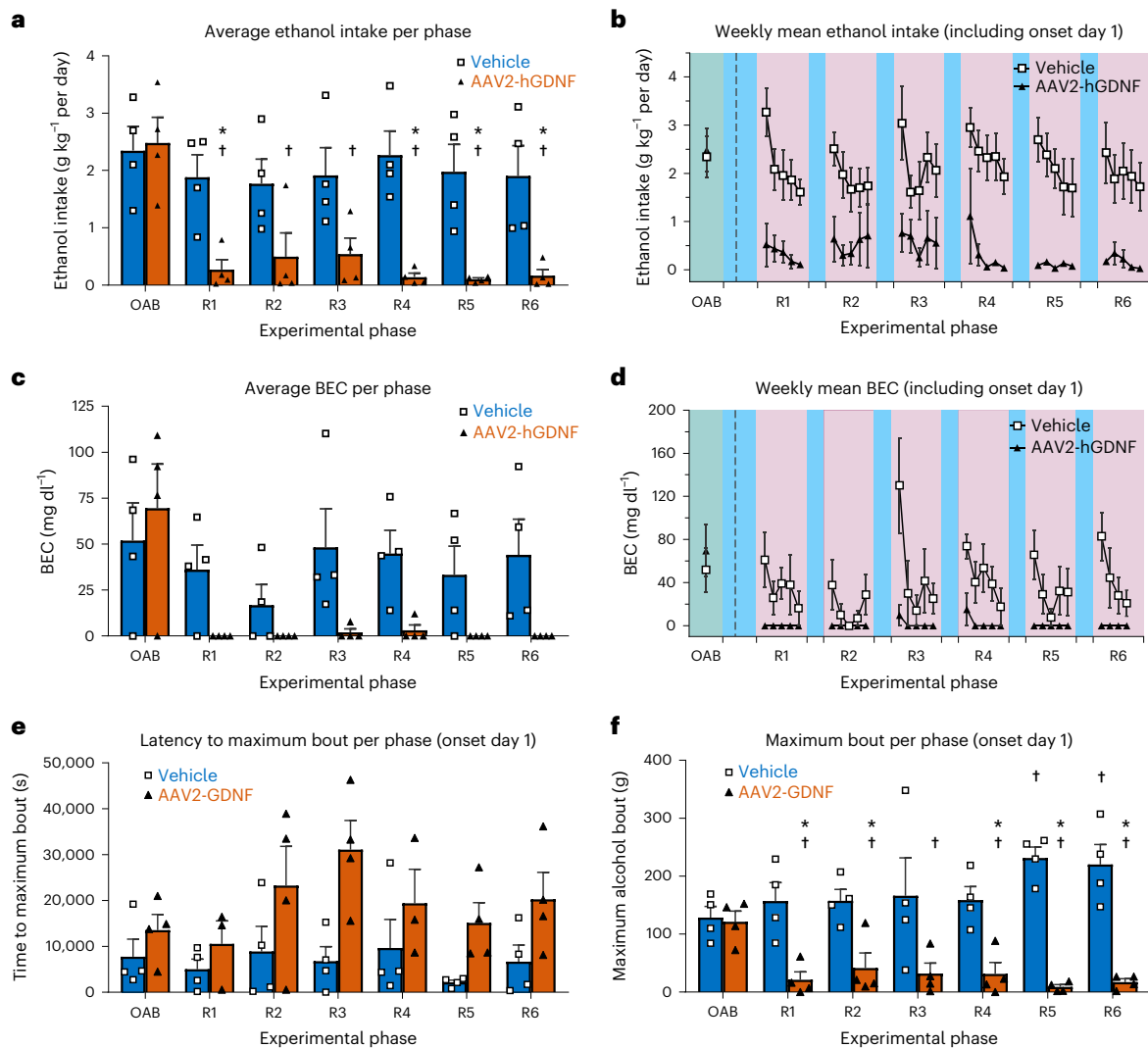


Fig. 3 | AAV2-hGDNF treatment curbs excessive drinking over a 1-year period.

a, b, Monthly (**a**) and weekly (**b**) group mean averages of daily alcohol intakes (grams per kilogram per day) from subjects by treatment group ($n = 4$ each) across each of the six alcohol reintroduction periods (R1–R6; mean \pm s.e.m., $n = 4$ /group; †: significant from within-group OAB value; *significant from respective vehicle group in phase (pairwise comparison using Student's two-sided t -test); R1 †, $P = 0.00374$, * $P = 0.00968$; R2 †, $P = 0.0176$; R3 †, $P = 0.0105$; R4 †, $P = 0.000209$, * $P = 0.00249$; R5 †, $P = 0.00183$, * $P = 0.00807$; and R6 †, $P = 0.00241$, * $P = 0.0182$). **c, d**, Monthly (**c**) and weekly (**d**) group means of BECs (milligrams per deciliter) from individual subjects by treatment group ($n = 4$ each) across all six reintroduction periods (R1–R6; mean \pm s.e.m., $n = 4$ /group).

e, f, Group means of latency to maximum alcohol intake bout (seconds) by treatment group (mean \pm s.e.m., $n = 4$ /group) on the day of onset for each reintroduction phase. **f**, Group means of the size of the maximum alcohol intake bout (milliliters) by treatment group on the day of onset for each alcohol reintroduction phase period (mean \pm s.e.m., $n = 4$ /group; †significant from within-group OAB value; *significant from respective vehicle group in phase (pairwise comparison using Student's two-sided t -test); vehicle: R5 †, $P = 0.00886$; and R6 †, $P = 0.05$; hGDNF: R1 †, $P = 0.00473$, * $P = 0.00779$; R2 †, $P = 0.0046$, * $P = 0.012$; R3 †, $P = 0.0132$; R4 †, $P = 0.0154$, * $P = 0.00057$; R5 †, $P = 0.00097$, * $P = 0.00003$; and R6 †, $P = 0.00166$, * $P = 0.00114$).

of AAV2-hGDNF-treated monkeys compared to vehicle-treated ($[t_{(df_6)} = 6.0, P \leq 0.001]$; Fig. 5c and Extended Data Fig. 5c). Levels of 3,4-dihydroxyphenylacetic acid (DOPAC) were 26.5-fold higher and levels of homovanillic acid (HVA) were 3-fold higher in AAV2-hGDNF-treated subjects relative to vehicle ($[t_{(df_6)} = 9.5, P \leq 0.001]$, $[t_{(df_6)} = 5.3, P \leq 0.01]$, respectively; Fig. 5d and Extended Data Fig. 5c), indicating significantly increased levels of DA and subsequent turnover associated with increased GDNF in the VTA.

In mesolimbic and mesocortical regions, DA levels appeared higher in the NAc and the caudate nucleus in three of the four GDNF-treated subjects compared to vehicle ($[t_{(df_6)} = 1.7, P = 0.15]$, $[t_{(df_6)} = 1.9, P \leq 0.10]$, respectively; Fig. 5c and Extended Data Fig. 5c). NAc, DOPAC and HVA levels were approximately 3-fold greater than in vehicle-treated subjects ($[t_{(df_6)} = 2.9, P \leq 0.05]$, $[t_{(df_6)} = 3.6, P \leq 0.05]$, respectively; Fig. 5d, e

and Extended Data Fig. 5c), and HVA was significantly elevated in the caudate nucleus, ventral putamen and cingulate gyrus (+3.7-fold, +2.5-fold, and +3-fold, respectively; Fig. 5e and Extended Data Fig. 5c). Levels of DA and its metabolites were unchanged in PFC. In substantia nigra, DA levels were unchanged, but DOPAC and HVA levels were significantly greater in AAV2-hGDNF subjects compared to vehicle ($[t_{(df_6)} = 4.7, P \leq 0.01]$, $[t_{(df_6)} = 4.1, P \leq 0.01]$, respectively; Fig. 5d, e). It is unclear whether this elevation is due to increased DA metabolism in the substantia nigra directly or extracellular metabolites from the neighboring VTA.

HVA/DA ratios, an index of DA utilization, were significantly increased in the NAc, putamen and CN of AAV2-hGDNF-treated monkeys as compared to vehicle-treated ($F_{2,17} = 21.6; P \leq 0.01$, $P \leq 0.001$ and $P \leq 0.05$, respectively; Fig. 5f). When compared to ratios in naïve

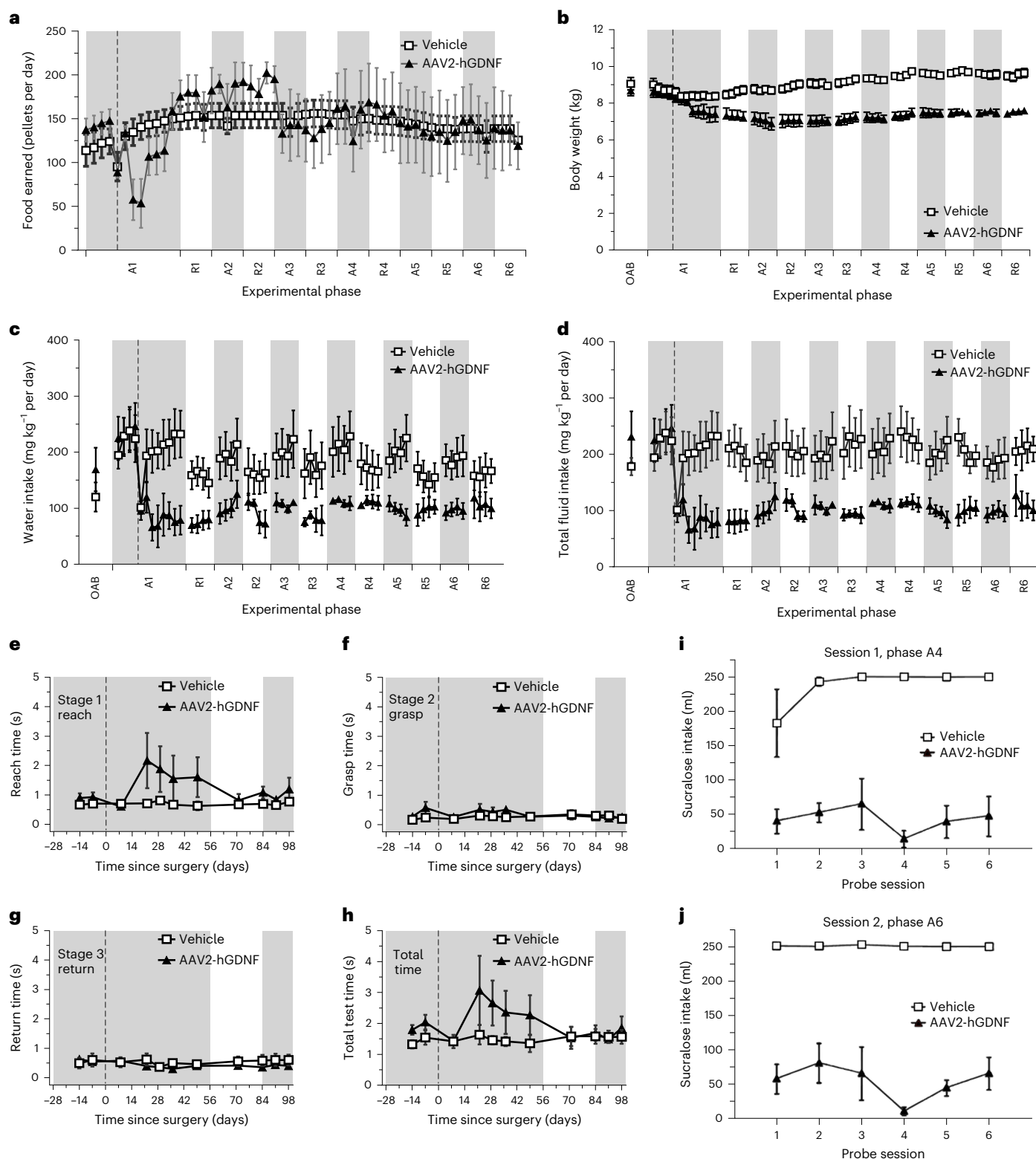


Fig. 4 | Effects of AAV2-hGDNF on food and water intake, weight, sensorimotor tasks and alternative reward motivation. **a**, Weekly averages of the daily food pellets earned by individual subjects (pellets/day), shown by group (mean \pm s.e.m.; AAV2-hGDNF, $n = 4$; vehicle, $n = 4$) across the study periods from A1 (starting 4 weeks before surgery) through R6 (52 weeks). **b**, Weekly averages of the individual subject weight (kg), shown by group (mean \pm s.e.m.; AAV2-hGDNF; vehicle; $n = 4$ per group) from the last week of OAB through R6. **c, d**, Weekly group averages water intake (c) and total fluid intake (d) by individual subjects normalized to subject weight (milliliters per kilogram), shown by group (mean \pm s.e.m.; AAV2-hGDNF; vehicle; $n = 4$ per group) from the last week of OAB through R6. **e–h**, Average times (sec) of the stages of the reward reach sensorimotor test (e, reach; f, grasp; g, return) and total test time (h) by individual subjects, shown by group (mean \pm s.e.m.; AAV2-hGDNF; vehicle; $n = 4$ per group), from 2 weeks before surgery through 2 weeks into the A2 period (98 days post-surgery). **i, j**, Average sucralose solution intake by group (mean \pm s.e.m.; AAV2-hGDNF; vehicle; $n = 4$ per group) across six probe sessions conducted at 2 weeks into periods A4 (i) and A6 (j).

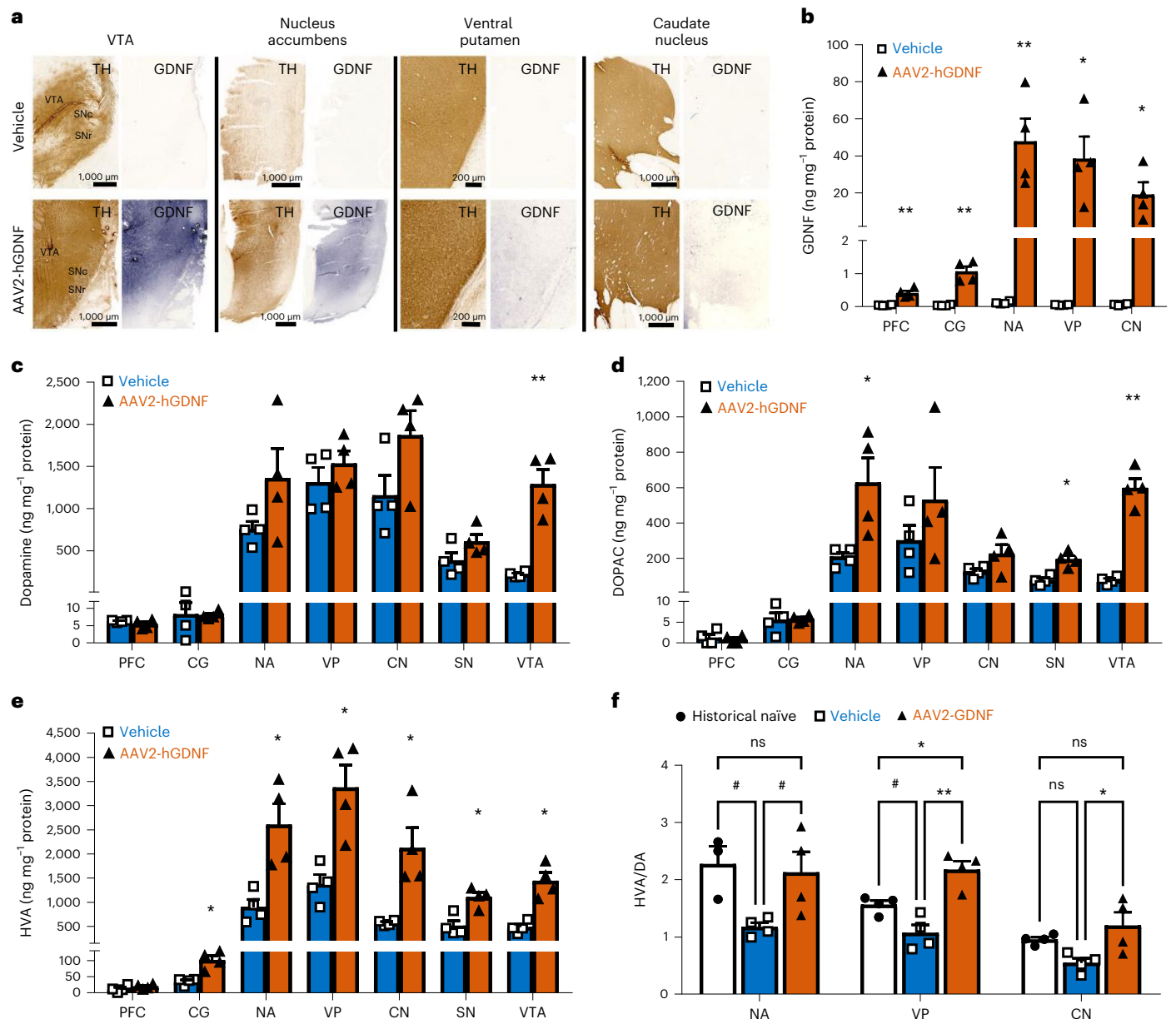


Fig. 5 | AAV2-hGDNF effects on GDNF expression, DA concentrations, and DA metabolism. **a**, Representative images of TH and GDNF protein immunohistochemistry in post-mortem tissue sections from midbrain (VTA), NAC, ventral putamen, and caudate nucleus in vehicle panel 4 macaque and AAV2-hGDNF panel 2 macaque (from three repeated immunochemical stains). **b**, The amount of GDNF protein measured in prefrontal cortex (PFC), cingulate gyrus (CG), nucleus accumbens (NA), ventral putamen (VP) and caudate nucleus (CN) from brain punch homogenates of vehicle-treated (blue) and AAV2-hGDNF-treated (orange) macaques determined by ELISA (nanograms per milligram protein) (mean \pm s.e.m.; $n = 4$ /group. PFC: $**P = 0.0016$; PFC: CG: $**P = 0.0006$; NA: $**P = 0.0088$; VP: $*P = 0.019$; CN: $*P = 0.029$; vs respective vehicle-treated control group value via two-tailed Student's *t*-test). **c–e**, Concentrations of DA (c) (VTA: $**P = 0.0010$) and its metabolites, 3,4-hihydroxyphenylacetic acid (d) (DOPAC; NA: $*P = 0.0275$; SN: $*P = 0.0034$; VTA: $*P = 0.0001$) and homovanillic

acid (e) (HVA; CG: $*P = 0.0039$; NA: $*P = 0.0108$; VP: $*P = 0.0082$; CN: $*P = 0.0102$; SN: $*P = 0.0064$; VTA: $*P = 0.0019$) in nanograms per milligram protein as determined by HPLC from tissue homogenates for macaques from each group (mean \pm s.e.m.; $n = 4$ /group. *P* value vs respective vehicle-treated control group value via two-tailed Student's *t*-test). **f**, Ratio of HVA to DA values from HPLC analyses (nanograms per milligram protein) for the NA, VP and CN from vehicle-treated (blue) and AAV2-hGDNF-treated (orange) macaques. Previously published HVA/DA values from naïve male rhesus macaques are provided as a historical naïve control (white)^{37–41} (mean \pm s.e.m.; $n = 3$ historical; $n = 4$ /study group. NA: #, $P = 0.0576$ historical vs vehicle, #, $P = 0.0744$ hGDNF vs vehicle; VP: #, $P = 0.0553$ historical vs vehicle, $*P = 0.0009$ historical vs hGDNF, $**P = 0.0005$ vehicle vs hGDNF; CN: $*P = 0.0267$ vehicle vs hGDNF; one-way analysis of variance (ANOVA) with Tukey's multiple comparisons test; ns, not significantly different vs respective group value).

rhesus monkeys from previously published data^{37–41}, DA utilization in vehicle-treated alcohol-drinking monkeys is significantly depressed in the NAC ($F_{2,17} = 21.6$; $P \leq 0.01$), and AAV2-hGDNF-treated monkeys exhibited HVA/DA ratios comparable with those of naïve primates (Fig. 5f). These results demonstrate target engagement of the GDNF transgene product with the DAergic neurons of the reward circuitry.

Levels of serotonin (5HT) and metabolite 5HIAA were also found to be increased by more than 2-fold in the VTA of GDNF-treated subjects as compared to vehicle-treated subjects ($t_{(df6)} = 2.7$, $P \leq 0.05$; $t_{(df6)} = 3.2$, $P \leq 0.05$; respectively) (Extended Data Fig. 5a–c). Notably, serotonergic changes play a role in VTA signaling and alcohol seeking behavior; 5HT and 5HIAA levels in the VTA are reduced following chronic alcohol use⁴².

AAV2-hGDNF affects accumbal DA signaling dynamics

Using *ex vivo* fast-scan cyclic voltammetry on NAc slices, we assessed alterations in stimulated DA release at terminals, using ‘tonic-like’ single-pulse stimulation and ‘phasic-like’ stimulation trains (10 pulses at increasing frequencies). Single-pulse DA release was not statistically significant between vehicle, AAV2-hGDNF, and housing control subjects ($F_{(2,9)} = 3.096$; $P = 0.0948$; Fig. 6a); however, three of the four vehicle-treated subjects exhibited lower single-pulse DA release compared to the mean of the AAV2-hGDNF-treated animals (mean = 0.2898). Both vehicle- ($P = 0.0057$) and AAV2-hGDNF-treated ($P = 0.0065$) groups had significantly slower DA reuptake than housing controls ($F_{(2,9)} = 11.61$; $P = 0.0032$; Fig. 6b), but there was no significant difference between vehicle- and AAV2-hGDNF-treated groups ($P = 0.9956$).

‘Phasic-like’ trains of stimulation, 10 pulses at 10, 20, 40 and 60 Hz, revealed a significant main effect of frequency ($F_{(3,45)} = 4.741$; $P = 0.0059$), a trend of group ($F_{(2,15)} = 2.778$; $P = 0.0941$) and a significant interaction ($F_{(6,45)} = 3.093$; $P = 0.0127$), such that vehicle-treated animals displayed the lowest ‘phasic-like’ release, housing controls exhibited the highest release, and AAV2-hGDNF-treated animals showed a partial reversal of alcohol-mediated inhibition of ‘phasic-like’ DA release (Fig. 6c). Though not significantly different, ‘phasic-like’ DA release was 1.8- to 2.5-fold higher in AAV2-hGDNF-treated vs vehicle-treated subjects across frequencies, suggesting a larger available pool of DA for potential release in the presynaptic terminals.

To assess acute effects of acute alcohol on DA release in the NAc, we bath applied physiologically relevant alcohol concentrations and recorded single-pulse stimulations. In vehicle-treated subjects, DA release was unaffected by bath application of alcohol ($F = 0.43$, $P = 0.66$; Fig. 6d). However, AAV2-hGDNF-treated subjects exhibited 30% and 46% lower DA release in response to 22-mM and 44-mM alcohol, respectively ($F = 4.23$, $P = 0.06$; Fig. 6e), suggesting increased sensitivity to acute inhibitory effects of alcohol at the presynaptic DA terminals.

Chronic alcohol sensitizes DAergic autoreceptors, resulting in greater inhibition of DA release in the presence of the D2/D3 DA receptor agonist, quinpirole^{9–11}. NAc slices were exposed to cumulative concentrations of quinpirole (30 nM, 100 nM). AAV2-hGDNF-treated subjects showed a reduced effect of quinpirole when compared to the vehicle group following single-pulse stimulation (Fig. 6f). A significant effect of quinpirole concentration ($F_{1,4} = 7.99$, $P \leq 0.05$) on DA release was observed, as well as a significant difference between AAV2-hGDNF- and vehicle-treated subjects at both concentrations ($F_{1,4} = 14.7$, $P \leq 0.05$).

Chronic exposure to alcohol increases the ability of kappa opioid receptor (KOR) agonists to inhibit DA release⁴³. We bath added cumulative concentrations of KOR agonist U50,488 (0.3 μ M, 1 μ M) and applied single-pulse stimulations. We observed no difference in response to U50,488 between AAV2-hGDNF- and vehicle-treated subjects (group: $F_{1,5} = 0.49$, $P = 0.51$; concentration: $F_{1,5} = 1.92$, $P = 0.22$; subjects: $F_{5,5} = 11.65$, $P = 0.0087$; interaction: $F_{1,5} = 0.03$, $P = 0.87$; Fig. 6g), indicating GDNF did not alter KOR function.

NAc nicotinic acetylcholine receptors (nAChRs) are implicated in alcohol-mediated DA reductions in response to ‘phasic-like’ stimulation trains, and nAChR antagonism can block the acute alcohol-mediated inhibition of DA release both *in vivo* and *ex vivo*^{44,45}. We examined DA release in response to single pulses and stimulation trains in the presence of the selective $\alpha 4$ subunit-containing nAChR antagonist dihydro- β -erythroidine hydrobromide (DH β E). Unlike the augmented phasic-like release of DA observed in the AAV2-hGDNF-treated subjects in drug-free conditions (Fig. 6c), with DH β E no significant difference was observed between AAV2-hGDNF and Vehicle-treated subjects as a percent of the single-pulse baseline ($F_{1,4} = 1.91$, $P = 0.24$; Fig. 6h), although there was a main effect of frequency ($F_{3,12} = 5.49$, $P \leq 0.05$). When analyzed as comparison of response to stimulation trains in DH β E normalized to baseline release prior to DH β E application, AAV2-hGDNF and vehicle-treated subjects seem to ‘normalize’; vehicle subjects had

an augmented response to stimulation trains, but AAV2-hGDNF subjects had an attenuated response (between groups, $F_{1,4} = 1.91$, $P = 0.10$; main effect of frequency, $F_{3,12} = 4.143$, $P \leq 0.05$; Fig. 6i), suggesting modulation of nAChRs by GDNF overexpression.

Discussion

In this study, we demonstrate that delivery of AAV2-hGDNF to the VTA of male NHP subjects in a chronic alcohol self-administration model significantly modified the DAergic signaling in the CNS reward system and ablated alcohol-intake patterns across six cycles of alcohol abstinence/reintroduction. This durable effect is key to overcoming the cycles of increased drinking following attempts at decreasing alcohol intake that current pharmacological therapies are prone to, while providing lasting change to the underlying DA signaling system dysfunction associated with AUD. While further work is needed to assure proper dosing for targeted treatment, these data demonstrate the promise of a one-time AAV2-hGDNF infusion after chronic daily alcohol drinking has been established to address the underlying neurophysiopathology and provide a much-needed treatment for patients with AUD.

In addition to lowering alcohol intakes, AAV2-hGDNF treatment restored DAergic function in the NAc. It has been documented that hypodopaminergia in the mesolimbic system follows chronic alcohol use^{9–12}. Clinical studies have also shown various measures of low DA the reward pathway after chronic alcohol use^{46,47}. We show that AAV2-hGDNF infusion augmented DA availability and utilization in the reward pathway of alcohol-drinking macaques to values comparable with alcohol-naïve macaques^{37–41}, suggesting that overexpression of GDNF in the VTA reversed or partially restored the imbalances in DAergic function associated with chronic alcohol consumption^{10,12}. This finding supports the role of GDNF as a key regulator of alcohol use via maintenance of mesolimbic DAergic function²⁴.

We emphasize this is a proof-of-concept study evaluating phenotypic effects in a well-characterized primate alcohol use model, in which we administered a high dose of vector to ensure target engagement. Indeed, we do observe altered regulation of DA. We also note that GDNF treatment did not appear to result in abhorrent DA terminal function, as we do not observe aberrant DA neuron signaling or utilization above naïve controls. Nevertheless, we must consider potential limitations, in particular the possibility of creating a hyperdopaminergic state. While beneficial in the setting of AUD, increased DA could be detrimental to other behaviors, such as stimulant use disorders, regulated by DA signaling of the mesolimbic system. Lu et al.⁴⁸ found that viral-mediated GDNF overexpression in the VTA led to an increase in cocaine relapse when the drug was reintroduced in 2–4 weeks following viral GDNF administration⁴⁸. Conversely, earlier studies demonstrated that enhancement of central GDNF-signaling counteracts neurochemical and behavioral responses to cocaine, methamphetamine, and opioids^{49,50}, though modulation appears to be brain site- and addiction-cycle-phase dependent. Further work is needed to ensure a beneficial effect while not risking triggering stimulant use disorders or other detrimental behaviors.

Previous studies evaluating viral-mediated GDNF expression in the midbrain of rodents and NHPs have also reported weight loss and transient behavioral disturbances, as observed here^{51–54}. Tümer et al.⁵³ and Manfredsson et al.⁵¹ suggested that weight loss observed in GDNF-treated rats may be associated with increased energy expenditure and activation of corticotrophin-releasing hormone neurons of the hypothalamus^{51,53}. In a human clinical trial studying intraventricular infusion of GDNF protein, patients exhibited average weight losses of 5%⁵⁵. Another factor to consider in our study is the loss of caloric intake from not consuming ethanol combined with similar food pellet intake between groups between phases A3–R6. Our results suggest the difference in weight may be a combination of the initial transient weight loss exhibited by the AAV2-hGDNF group followed by a lower total caloric intake during the alcohol reintroduction periods as compared to the

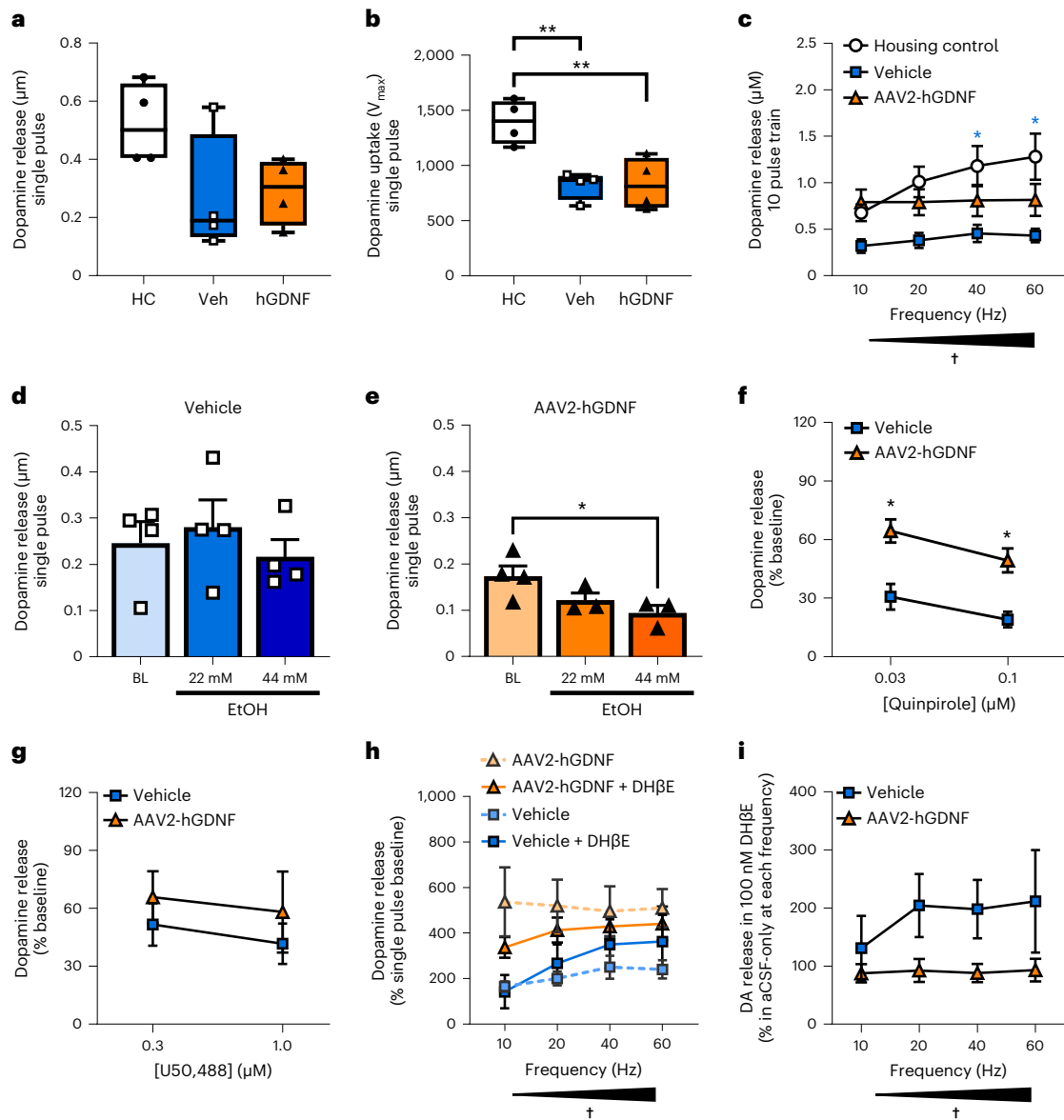


Fig. 6 | AAV2-hGDNF treatment alters dopaminergic neuron dynamics and modulation in the NAc. **a**, Stimulated DA evoked by single-pulse stimulation in housing control (HC) animals in comparison to AAV2-hGDNF- or vehicle-treated animals (mean \pm s.e.m.; $n = 4$ /group). **b**, The maximal rate of DA uptake (V_{max}) in HC animals in comparison to AAV2-hGDNF- or vehicle-treated animals (box plots: median values with whiskers indicating minimum to maximum values; symbols indicate individual subject values, $n = 4$ /group; HCs vs vehicle, $**P = 0.0057$; HCs vs hGDNF, $**P = 0.0065$ via one-way ANOVA with Tukey's multiple comparisons test). **c**, DA release elicited by stimulation trains of 10 pulses at increasing frequencies (mean \pm s.e.m.; $n = 4$ /group; for housing control vs vehicle at 40 Hz $*P = 0.0400$, 60 Hz $*P = 0.0136$; †: main effect of frequency, $P = 0.0059$; two-way ANOVA with Tukey's multiple comparisons test). **d, e**, Effect of ethanol (EtOH) applied over NAc slices at increasing concentrations (22 mM, 44 mM) on single-pulse stimulated release in vehicle-treated subjects as compared to baseline (BL) drug-free artificial cerebrospinal fluid (aCSF) conditions (mean \pm s.e.m.;

$n = 4$ /group) (**d**) and in AAV2-hGDNF subjects compared to BL (**e**) (mean \pm s.e.m.; $n = 4$ /BL, $n = 3$ /22 mM and 44 mM EtOH; BL vs 22 mM, $\#P = 0.1081$; BL vs 44 mM, $*P = 0.0257$ via one-way ANOVA with Fisher's LSD). **f**, DA autoreceptor sensitivity to the D2/D3 agonist quinpirole (0.03, 0.1 µM) in vehicle and AAV2-hGDNF subjects (mean \pm s.e.m.; $n = 4$ /group; 0.03 µM $*P = 0.0160$, 0.1 µM $*P = 0.0265$ via two-way ANOVA with Sidak's multiple comparisons test). **g**, DA release inhibition by the kappa opioid receptor agonist U50,488 at increasing doses. (mean \pm s.e.m.; $n = 4$ /group). **h**, DA release with trains of stimulation at increasing frequencies in the absence or presence of the nicotinic acetylcholine receptor antagonist DHβE (100 mM) as normalized to percentage of DA release at a single-pulse baseline († = main effect of frequency, $P = 0.0198$). **i**, DA release with trains of stimulation at increasing frequencies in the presence of DHβE (100 mM) as normalized to percent of DA release in aCSF alone at each frequency prior to DHβE († = main effect of frequency, $P = 0.0155$, mean \pm s.e.m.; $n = 4$ /group).

vehicle-treated group. AAV2-hGDNF-treated macaques also exhibited a decreased avidity to consume a sucralose-sweetened solution reward. Although the reduction could be interpreted as generalized anhedonia, this contrasts with the regain of normal food intake and performance on the raisin reach-and-grasp sensorimotor task. These results suggest the decreased pursuit of an alternate reward was not pure loss of

motivation nor aversion, but rather complex regulation of the reward pathway in GDNF-treated subjects.

The use of gene therapy for treating CNS disorders is an established and rapidly expanding field. MR-guided VTA delivery of AAV2 vector has been demonstrated to be safe and tolerable in macaques at comparable doses³⁰, and has been safely utilized in the midbrain

in human patients⁵⁶. The safety of intraparenchymal AAV2-hGDNF delivery and expression has also been demonstrated in NHP, and putaminal delivery of AAV2-hGDNF is currently being evaluated as a treatment for PD in clinical trials (NCT04167540, NCT01621581)^{38,52,57–60}. Given the profound efficacy of GDNF gene therapy to mitigate reintroduction-associated alcohol intake in our NHP model, we believe that this therapeutic approach could be a promising therapy for AUD, and possibly have efficacy to other substance use disorders.

Online content

Any methods, additional references, Nature Portfolio reporting summaries, source data, extended data, supplementary information, acknowledgements, peer review information; details of author contributions and competing interests; and statements of data and code availability are available at <https://doi.org/10.1038/s41591-023-02463-9>.

References

- Sacks, J. J., Gonzales, K. R., Bouchery, E. E., Tomedi, L. E. & Brewer, R. D. 2010 national and state costs of excessive alcohol consumption. *Am. J. Prev. Med.* **49**, e73–e79 (2015).
- Substance Abuse and Mental Health Services Administration. Key substance use and mental health indicators in the United States: Results from the 2017 national survey on drug use and health recommended citation substance abuse and mental health services administration. HHS Publication No. SMA 18-53 (2018).
- Kanny, D., Naimi, T. S., Liu, Y. & Brewer, R. D. Trends in total binge drinks per adult who reported binge drinking—United States, 2011–2017. *MMWR Morb. Mortal. Wkly. Rep.* **69**, 30–34 (2020).
- Witkiewitz, K. et al. Advances in the science and treatment of alcohol use disorder. *Sci. Adv.* **5**, eaax4043 (2019).
- Gueorguieva, R., Wu, R., Krystal, J. H., Donovan, D. & O'Malley, S. S. Temporal patterns of adherence to medications and behavioral treatment and their relationship to patient characteristics and treatment response. *Addict. Behav.* **38**, 2119–2127 (2013).
- Koob, G. F. Theoretical frameworks and mechanistic aspects of alcohol addiction: alcohol addiction as a reward deficit disorder. *Curr. Top. Behav. Neurosci.* **13**, 3–30 (2011).
- Volkow, N. D., Wang, G. J., Fowler, J. S. & Tomasi, D. Addiction circuitry in the human brain. *Annu. Rev. Pharmacol. Toxicol.* **52**, 321–336 (2012).
- Charlet, K., Beck, A. & Heinz, A. The dopamine system in mediating alcohol effects in humans. *Curr. Top. Behav. Neurosci.* **13**, 461–488 (2011).
- Karkhanis, A. N., Rose, J. H., Huggins, K. N., Konstantopoulos, J. K. & Jones, S. R. Chronic intermittent ethanol exposure reduces presynaptic dopamine neurotransmission in the mouse nucleus accumbens. *Drug Alcohol Depend.* **150**, 24–30 (2015).
- Siciliano, C. A. et al. Increased presynaptic regulation of dopamine neurotransmission in the nucleus accumbens core following chronic ethanol self-administration in female macaques. *Psychopharmacol.* **233**, 1435–1443 (2016).
- Siciliano, C. A. et al. Chronic ethanol self-administration in macaques shifts dopamine feedback inhibition to predominantly D2 receptors in nucleus accumbens core. *Drug Alcohol Depend.* **158**, 159–163 (2016).
- Siciliano, C. A., Karkhanis, A. N., Holleran, K. M., Melchior, J. R. & Jones, S. R. Cross-species alterations in synaptic dopamine regulation after chronic alcohol exposure. *Handb. Exp. Pharmacol.* **248**, 213–238 (2018).
- Thanos, P. K. et al. Overexpression of dopamine D2 receptors reduces alcohol self-administration. *J. Neurochem.* **78**, 1094–1103 (2001).
- Airaksinen, M. S. & Saarma, M. The GDNF family: signalling, biological functions and therapeutic value. *Nat. Rev. Neurosci.* **3**, 383–394 (2002).
- Barak, S. et al. Positive autoregulation of GDNF levels in the ventral tegmental area mediates long-lasting inhibition of excessive alcohol consumption. *Transl. Psychiatry* **1**, e60 (2011).
- Barak, S., Carnicella, S., Yowell, Q. V. & Ron, D. Glial cell line-derived neurotrophic factor reverses alcohol-induced allostasis of the mesolimbic dopaminergic system: implications for alcohol reward and seeking. *J. Neurosci.* **31**, 9885–9894 (2011).
- Lin, L.-F., Doherty, D. H., Lile, J. D., Bektesh, S. & Collins, F. GDNF: A glial cell line-derived neurotrophic factor for midbrain dopaminergic neurons. *Science* **260**, 1130–1132 (1993).
- Ahmadiantehrani, S., Barak, S. & Ron, D. GDNF is a novel ethanol-responsive gene in the VTA: implications for the development and persistence of excessive drinking. *Addict. Biol.* **19**, 623–633 (2014).
- Heberlein, A. et al. BDNF and GDNF serum levels in alcohol-dependent patients during withdrawal. *Prog. Neuropsychopharmacol. Biol. Psychiatry* **34**, 1060–1064 (2010).
- Barak, S. et al. Glial cell line-derived neurotrophic factor (GDNF) is an endogenous protector in the mesolimbic system against excessive alcohol consumption and relapse. *Addict. Biol.* **20**, 626–642 (2015).
- Wang, J. et al. Nucleus accumbens-derived glial cell line-derived neurotrophic factor is a retrograde enhancer of dopaminergic tone in the mesocorticolimbic system. *J. Neurosci.* **30**, 14502–14512 (2010).
- Carnicella, S., Amamoto, R. & Ron, D. Excessive alcohol consumption is blocked by glial cell line-derived neurotrophic factor. *Alcohol* **43**, 35–43 (2009).
- Carnicella, S., Kharazia, V., Jeanblanc, J., Janak, P. H. & Ron, D. GDNF is a fast-acting potent inhibitor of alcohol consumption and relapse. *Proc. Natl Acad. Sci. USA* **105**, 8114–8119 (2008).
- Barak, S., Ahmadiantehrani, S., Logrip, M. L. & Ron, D. GDNF and alcohol use disorder. *Addict. Biol.* **24**, 335–343 (2019).
- Grant, K. A. et al. Drinking typography established by scheduled induction predicts chronic heavy drinking in a monkey model of ethanol self-administration. *Alcohol Clin. Exp. Res.* **32**, 1824–1838 (2008).
- Allen, D. C., Gonzales, S. W. & Grant, K. A. Effect of repeated abstinence on chronic ethanol self-administration in the rhesus monkey. *Psychopharmacology* **235**, 109–120 (2018).
- Cuzon Carlson, V. C. et al. Synaptic and morphological neuroadaptations in the putamen associated with long-term, relapsing alcohol drinking in primates. *Neuropsychopharmacology* **36**, 2513–2528 (2011).
- National Institute on Alcohol Abuse and Alcoholism NIAAA council approves definition of binge drinking. *NIAAA Newsl.* **3**, 3 (2004).
- Sudhakar, V. et al. Development of a novel frameless skull-mounted ball-joint guide array for use in image-guided neurosurgery. *J. Neurosurg.* **132**, 595–604 (2020).
- Sebastian, W. S. et al. Safety and tolerability of MRI-guided infusion of AAV2-hAADC into the mid-brain of nonhuman primate. *Mol. Ther. Methods Clin. Dev.* **3**, 14049 (2014).
- Ciesielska, A. et al. Anterograde axonal transport of AAV2-GDNF in rat basal ganglia. *Mol. Ther.* **19**, 922–927 (2011).
- Becker, H. C. Kindling in alcohol withdrawal. *Alcohol Health Res. World* **22**, 25–33 (1998).
- Summers, L., Clingerman, K. J. & Yang, X. Validation of a body condition scoring system in rhesus macaques (*Macaca mulatta*): assessment of body composition by using dual-energy X-ray absorptiometry. *J. Am. Assoc. Lab Anim. Sci.* **51**, 88–93 (2012).
- Labberton, L., Bakker, J., Klomp, R., Langermans, J. A. & van Geijlswijk, I. M. Challenges in oral administration of metronidazole dissolved in drinking water to rhesus monkeys (*Macaca mulatta*). *Lab Anim.* **42**, 213–216 (2013).

35. Yamada, H., Louie, K. & Glimcher, P. W. Controlled water intake: a method for objectively evaluating thirst and hydration state in monkeys by the measurement of blood osmolality. *J. Neurosci. Methods* **191**, 83–89 (2010).
36. Barnes, S. A., Der-Avakian, A. & Markou, A. Anhedonia, avolition, and anticipatory deficits: assessments in animals with relevance to the negative symptoms of schizophrenia. *Eur. Neuropsychopharmacol.* **24**, 744–758 (2014).
37. Burns, R. S. et al. A primate model of parkinsonism: selective destruction of dopaminergic neurons in the pars compacta of the substantia nigra by N-methyl-4-phenyl-1,2,3,6-tetrahydropyridine. *Proc. Natl Acad. Sci. USA* **80**, 4546–4550 (1983).
38. Johnston, L. C. et al. Clinically relevant effects of convection-enhanced delivery of AAV2-GDNF on the dopaminergic nigrostriatal pathway in aged rhesus monkeys. *Hum. Gene Ther.* **20**, 497–510 (2009).
39. Oiwa, Y. et al. Overlesioned hemiparkinsonian non human primate model: correlation between clinical, neurochemical and histochemical changes. *Front. Biosci.* **8**, a155–a166 (2003).
40. Pifl, C., Bertel, O., Schingnitz, G. & Hornykiewicz, O. Extrastriatal dopamine in symptomatic and asymptomatic rhesus monkeys treated with 1-methyl-4-phenyl-1,2,3,6-tetrahydropyridine (MPTP). *Neurochem. Int.* **17**, 263–270 (1990).
41. Pifl, C., Schingnitz, G. & Hornykiewicz, O. The neurotoxin MPTP does not reproduce in the rhesus monkey the interregional pattern of striatal dopamine loss typical of human idiopathic Parkinson's disease. *Neurosci. Lett.* **92**, 228–233 (1988).
42. Sari, Y., Johnson, V. R. & Weedman, J. M. Role of the serotonergic system in alcohol dependence: from animal models to clinics. *Prog. Mol. Biol. Transl. Sci.* **98**, 401–443 (2011).
43. Karkhanis, A., Holleran, K. M. & Jones, S. R. *Dynorphin/Kappa Opioid Receptor Signaling in Preclinical Models of Alcohol, Drug, and Food Addiction* 1st edn (Elsevier, 2017).
44. Schilaty, N. D. et al. Acute ethanol inhibits dopamine release in the nucleus accumbens via $\alpha 6$ nicotinic acetylcholine receptors. *J. Pharmacol. Exp. Ther.* **349**, 559–567 (2014).
45. Yorgason, J. T., Rose, J. H., McIntosh, J. M., Ferris, M. J. & Jones, S. R. Greater ethanol inhibition of presynaptic dopamine release in C57BL/6J than DBA/2J mice: role of nicotinic acetylcholine receptors. *Neuroscience* **284**, 854–864 (2015).
46. Martinez, D. et al. Alcohol dependence is associated with blunted dopamine transmission in the ventral striatum. *Biol. Psychiatry* **58**, 779–786 (2005).
47. Volkow, N. D. et al. Profound decreases in dopamine release in striatum in detoxified alcoholics: possible orbitofrontal involvement. *J. Neurosci.* **27**, 12700–12706 (2007).
48. Lu, L. et al. Role of ventral tegmental area glial cell line-derived neurotrophic factor in incubation of cocaine craving. *Biol. Psychiatry* **66**, 137–145 (2009).
49. Carnicella, S. & Ron, D. GDNF – a potential target to treat addiction. *Pharmacol. Ther.* **122**, 9–18 (2009).
50. Messer, C. J. et al. Role for GDNF in biochemical and behavioral adaptations to drugs of abuse. *Neuron* **26**, 247–257 (2000).
51. Manfredsson, F. P. et al. Nigrostriatal rAAV-mediated GDNF overexpression induces robust weight loss in a rat model of age-related obesity. *Mol. Ther.* **17**, 980–991 (2009).
52. Su, X. et al. Safety evaluation of AAV2-GDNF gene transfer into the dopaminergic nigrostriatal pathway in aged and parkinsonian rhesus monkeys. *Hum. Gene Ther.* **20**, 1627–1640 (2009).
53. Tümer, N. et al. Hypothalamic rAAV-mediated GDNF gene delivery ameliorates age-related obesity. *Neurobiol. Aging* **27**, 459–470 (2006).
54. Kells, A. P., Forsayeth, J. & Bankiewicz, K. S. Glial-derived neurotrophic factor gene transfer for Parkinson's disease: anterograde distribution of AAV2 vectors in the primate brain. *Neurobiol. Dis.* **48**, 228–235 (2012).
55. Nutt, J. G. et al. Randomized, double-blind trial of glial cell line-derived neurotrophic factor (GDNF) in PD. *Neurology* **60**, 69–73 (2003).
56. Pearson, T. S. et al. Gene therapy for aromatic L-amino acid decarboxylase deficiency by MR-guided direct delivery of AAV2-AADC to midbrain dopaminergic neurons. *Nat. Commun.* **12**, 4251 (2021).
57. *AAV2-GDNF for Advanced Parkinson's Disease* (National Institute of Neurological Disorders and Stroke, 2023); www.clinicaltrials.gov
58. *GDNF Gene Therapy for Parkinson's Disease* (Brain Neurotherapy Bio, Inc., 2023); www.clinicaltrials.gov
59. Richardson, R. M. et al. Interventional MRI-guided putaminal delivery of AAV2-GDNF for a planned clinical trial in Parkinson's disease. *Mol. Ther.* **19**, 1048–1057 (2011).
60. Terse, P. S., Kells, A. P., Noker, P., Wright, J. F. & Bankiewicz, K. S. Safety assessment of AAV2-hGDNF administered via intracerebral injection in rats for treatment of Parkinson's disease. *Int. J. Toxicol.* **40**, 4–14 (2021).

Publisher's note Springer Nature remains neutral with regard to jurisdictional claims in published maps and institutional affiliations.

Springer Nature or its licensor (e.g. a society or other partner) holds exclusive rights to this article under a publishing agreement with the author(s) or other rightsholder(s); author self-archiving of the accepted manuscript version of this article is solely governed by the terms of such publishing agreement and applicable law.

© The Author(s), under exclusive licence to Springer Nature America, Inc. 2023

Methods

Statement of research compliance with relevant ethical regulations

The current study involving experimental work with rhesus macaques was approved by the Institutional Animal Care and Usage Committee (IACUC) operating at the Oregon National Primate Research Center, Oregon Health & Science University. All surgical, treatment and husbandry decisions were made in consultation with experienced NHP veterinarian staff to ensure the well-being of animal subjects, and were approved by the IACUC. Additional regulatory oversight for the use of an adeno-associated viral vector encoding human glial cell-derived neurotrophic factor (AAV2-GDNF) in live animals was provided by the Institutional Biosafety Committee (IBC) at Oregon Health & Science University. All procedures were performed in accord with NIH guidelines on the care and use of laboratory subjects.

Animal selection, acclimation and training

Eight male rhesus macaque monkeys (aged 5.1 ± 0.2 y, weight 7.1 ± 0.3 kg) were recruited for this study. The vast majority of the historical data cited in support of this study was generated in male rhesus monkeys, and so use of males provided direct validation of our model and demonstrates the translational advantages of the current studies that were also run in male subjects. No statistical methods were used to predetermine sample sizes but our sample sizes are similar to those reported in previous publications^{25–27,61,62}. Macaque subjects conditioned at this young age (human equivalent of 19–23 y) are strongly disposed to develop heavy drinking behavior⁶¹. Seven of the subjects were born at the Oregon National Primate Research Center (ONPRC) and one subject was acquired from the New England Primate Research Center approximately 2 y before project assignment. Subjects were placed under a 12-h/12-h light/dark cycle and single-housed in quad cage racks that permit visual and auditory inspection of neighboring subjects during experimental sessions. Subjects were also socially paired for 2 h per day between sessions. Food consisted of nutritionally complete 1 g banana-flavored pellets (63% carbohydrate, 4% fat, and 22% protein; TestDiet, 1811182) and fresh fruit. Over an ensuing 3-month period (17 weeks), subjects were acclimated to a food-pellet-only diet and trained to present a leg to provide experimenter access to a femoral vein for blood sampling in an un-sedated state²⁵. During the final month of acclimation, a panel was mounted on each cage with two drinking spouts (Lixit valves), a three-light array (green, white, red) above each spout, a bar pull, a finger poke device, a food dispenser and a receptacle for delivery of the 1 g banana-flavored pellets. Subjects were trained to operate panel components to acquire food (bar pull plus finger poke) and water (bar pull plus spout-displacement). Unlimited access to water was provided except during active induction sessions. All collected observational and analog data points were organized using Microsoft Excel spreadsheet software.

Induction of chronic alcohol binge drinking

Initiation of alcohol drinking involved four 30-day epochs of schedule-induced drinking with water and then three increasing volumes (doses) of alcohol (Fig. 1a,b). A 4% w/v alcohol solution was presented and standard induction doses of 0.5, 1.0 and 1.5 g kg^{-1} per day were used, corresponding to volumes of 92 ± 4 , 196 ± 14 and 297 ± 12 ml, respectively. Schedule-induced polydipsia was carried out by placing subjects under a fixed schedule of food reinforcement in which a pellet was delivered every 5 min in the presence of alcohol²⁵. In brief, white stimulus lights were illuminated to signal active schedule and panel. The green stimulus light above the 'alcohol' spout was also on while the schedule was in effect to orient the subject's attention towards the alcohol. Side placement of the 'alcohol' spout was counterbalanced across subjects. Once the target volume (that is, dose) was consumed, the green stimulus light was extinguished and the schedule terminated. After a 2-h timeout, unrestricted access to water was permitted through

panel operation. Concurrently, daily food ration (pellet delivery) was also available contingent on a FRI schedule of responding on the finger poke device. Blood samples were collected weekly 90 min into an induction session to measure BEC²⁵ and reflect time to peak BEC as previously determined following nasogastric gavage of macaques with the 1.5 g kg^{-1} alcohol dose⁶².

OAB drinking

Following the induction of binge drinking, subjects had ad libitum access to both alcohol and water. Daily drinking sessions were 21 h long and were maintained over 6 months (27 weeks) to develop heavy drinking patterns (Fig. 1a,b). Pellet rations were divided into three daily meals administered through the instrumental panel during beginning, hour 4 and hour 6 of each session. Blood samples were collected weekly at approximately hour 7 into a drinking session (immediately prior to lights out) to measure BEC and monitor the physiological relevance of daytime alcohol self-administration²⁵.

Abstinence 1 (A1) period

At the conclusion of the OAB phase, abstinence was imposed (Fig. 1a), whereby alcohol was removed and water was presented from both fluid spouts^{26,27}. A1 lasted 12 weeks, and AAV2-hGDNF treatment was performed at week 4, followed by the remaining additional 8 weeks for surgical recovery and transgene expression. A series of behavioral observations were conducted 6 days before and 0, 1, 2, 3, 7, 14 and 21 days after abstinence onset as a baseline pre-surgery observation. Then, post-surgical observations were performed at least every 2 weeks over an ensuing 3-month period to quantify behavioral consequences associated with abstinence and/or GDNF overexpression. During these series, each subject was monitored for a period of 15 min, and at the conclusion of each observation period, a separate raisin-reach test was performed to assess fine motor skills⁶³.

Group assignments

Four weeks after phase A1 initiation, study subject macaques were assigned to one of two treatment groups, counterbalanced for average grams per kilogram per day alcohol intake during the final 7 days of the OAB phase (Fig. 1e). GDNF-treated subjects ($n = 4$) were infused with AAV2-hGDNF at a concentration of $2.0 \times 10^{13} \text{ vg ml}^{-1}$ in a volume of 30 μl , with doses given bilaterally into the VTA under MR imaging (MRI)-guided CED with a stepped catheter (ClearPoint Neuro) and transfrontal trajectory. Vehicle subjects ($n = 4$) received sterile phosphate-buffered saline spiked with ProHance H following the same procedure. Prior to the experimental study, a pilot study with two (2) male rhesus macaques was undertaken utilizing the described methods to optimize the volume and targeted delivery of AAV2-GFP to the VTA with MRI guidance (Extended Data Fig. 2). MR-guided CED was carried out following previously described methodology^{38,64,65}, as further detailed below.

MRI acquisition

MR images were acquired on a 3-Tesla Siemens Magnetom Trio scanner (Siemens Medical Solutions) using a CP Body Array Flex 63 Coil placed beneath the animal's head and around the body. MR images were acquired using previously established methods and are described here briefly. Three-dimensional, T1, magnetization-prepared and rapid gradient echo (3D-MP-RAGE) images were obtained with repetition time = 2,500 ms, echo time = 2.92 ms, flip angle = 9° , number of excitations = 1, matrix = 256×147 , field of view = $240 \times 240 \times 240$, and slice thickness = 1 mm. These parameters resulted in a 1-mm^3 voxel volume. An MP-RAGE imaging protocol was used to acquire high-resolution images to optimize visualization of brain structures during trajectory planning and to determine placement of the infusion catheter within the ball-joint guide cannula array. A modified T1-weighted protocol was used to obtain a rapid scan to assess vector spread. The number

of slices varied depending on the extent of infusate distribution and the scan time ranged from 5 to 10 min.

Surgical implantation

Surgery procedures were performed on the day of intracerebral dosing at the Oregon National Primate Research Center, OHSU, in accordance to IACUC requirements. After induction anesthesia, the animal's head was shaved, secured onto an MRI-compatible stereotactic frame and placed in the prone position. A sterile field was created and a midline incision was performed through the skin, muscle, and fascia using aseptic techniques. Gentle retraction of fascia and muscle allowed for cranial exposure. Two small burr holes were created in the transfrontal region of the skull while leaving the underlying dura intact. Customized ball-joint guidance arrays (BJGA) were placed over each craniotomy site and consisted of a base (attached to the skull using titanium screws), a guide tube array (cylinder with three holes), and an MRI visible fiducial filled with gadolinium. The wound site was closed in anatomical layers around the BJGA and a sterile adhesive (Ioban, 3M) was positioned over the skin to maintain sterility. The implanted animal was transferred to the MRI scanner, where baseline images were acquired for trajectory planning.

Infusion system and trajectory planning

The infusion system was prepared in the MRI suite and included (i) a custom-designed 16-gauge reflux-resistant cannula with a fused silica tip and ceramic shaft, (ii) a loading line containing AAV vector or phosphate-buffered saline (PBS) that was admixed with a gadolinium-based MR contrast agent diluted to a final concentration of 2 mM (ProHance H; Bracco Diagnostics)⁶⁵, and (iii) an infusion line containing PBS solution. The flow was regulated by a 3-mL syringe mounted onto an MRI-compatible infusion pump (Harvard Apparatus). After manually priming the system, the infusion rate was set at 1 to 3 $\mu\text{L min}^{-1}$ to maintain positive pressure and remove any air bubbles. Planning was performed on the MRI console using Siemens neuro-navigational software to visualize gadolinium signal in each fiducial placed in the BJGA. An optimal trajectory was determined by aligning the fiducial column to the VTA and acquiring T1 images to verify each adjustment. After identifying the proper access hole in the BJGA, a trajectory line was drawn from the target to the top of the guide stem. Using aseptic techniques, the surgeon measured the insertion distance from the tip of the fused silica cannula and secured a depth stop to the ceramic shaft. An MRI-compatible lancet was introduced through the selected guidance port on the BJGA stem to pierce the dura.

MRI-guided infusion procedure

Animals received one or two infusions per side of the brain that targeted the VTA. The infusion rate was set 3 $\mu\text{L min}^{-1}$ to prevent occlusion at the cannula tip as it was manually advanced through the BJGA to a region superior to the target. A T1 image was acquired to confirm the cannula tip location and ensure the trajectory aligned with the target. After advancing the cannula into the VTA, infusions proceeded at an initial rate of 1 $\mu\text{L min}^{-1}$ for 10 min followed by a rate of 2 $\mu\text{L min}^{-1}$ for 10 min. Scans were obtained through the infusion procedure to visualize vector spread and make cannula depth adjustments. After delivering a 30 μL volume, the cannula was removed and the procedure repeated on the contralateral hemisphere. Following intracerebral dosing, the animal was returned to surgery, the guidance devices explanted, and the wound site closed in anatomical layers. Subjects were monitored for full recovery from anesthesia and returned to their home-cage. The animal received an intramuscular injection of NSAID (Meloxicam) and buprenorphine (Buprenex) the day after the CED infusion as part of the post-procedural analgesia management. Veterinary staff performed daily cageside observations and provided supportive care during the post-surgery recovery period. Behavioral testing was initiated approximately 8 weeks later to evaluate the first alcohol reintroduction period (R1 in Fig. 1a).

Abstinence–alcohol reintroduction cycles

Alcohol was reintroduced at 8 weeks after surgery, and alcohol intake was monitored during six periods of 1 month each open alcohol access (alcohol reintroduction) (R1→R6 in Fig. 1a), interposed by five 1-month periods of force alcohol abstinence (A2→A6 in Fig. 1a). Escalation in alcohol intake after periods of withdrawal has been observed in humans^{6,66,67}, NHPs²⁶, rats⁶⁸ and mice⁶⁹. Further, duration and magnitude of this uncontrollable drinking are thought to progressively worsen as a factor of withdrawal experiences^{68,69}. A BEC sample was taken on the day of alcohol reintroduction onset and then weekly during each reintroduction phase. Similar to the A1 phase described above, behavioral observations were made during phases A2–A6 on day 0, 1, 3, 7, 14 and 21 following abstinence onset. Additional observations were made 14 days into each alcohol reintroduction phase.

Analysis of alcohol intake

Two primary dependent variables during 'open alcohol access' conditions were alcohol intake (grams per kilogram per day) and BEC (milligrams per deciliter). In addition, real-time consumption patterns of alcohol and water were recorded by measuring the mass displacement from each fluid reservoir in a time-stamped fashion via National Instruments hardware and LabView software. Custom, published programming scripts were implemented to analyze drinking pattern structure based on 'drink' and 'bout' units^{25,70,71}. Briefly, a drink was defined as continuous fluid consumption with less than a 5-s pause, whereas a bout reflected ongoing drinking with less than a 5-min pause. From these unit measures, drinking variables such as mean bout size and bout frequency were derived to model the metrics humans use to self-report their consumption levels⁷². Subjects were weighed weekly to facilitate calculation of alcohol consumed, and a detailed alcohol drinking phenotype was constructed for each subject from a composite of variables including grams per kilogram alcohol intake, BEC and drinking patterns.

Side reversal of alcohol spout

Alternate presentation of the alcohol spout was assessed to test perseveration to a fixed side bias. This procedure was modified from an earlier study examining drug reinforcement in mice⁷³. During the first 2 weeks of phase R3 (Fig. 1a), alcohol spouts were offered on the side opposite to their original position for all subjects to determine whether the amount of alcohol consumed was influenced by the side from which it was offered. Alcohol spouts were returned to their original positions for the last two weeks of phase R3 and the remainder of the study, with one exception. One GDNF-treated subject, panel 7, was maintained with the alcohol spout kept on the 'reversed' side because it developed an absolute side preference unrelated to the motivation to consume alcohol (Extended Data Fig. 4e–l). The reversal ensured continued water access and continued testing of alcohol preference for this subject.

Sucralose probe tests

Presentation of a sweet, highly-palatable solution was used to test the motivational state of study subjects, and to contrast the influence of AAV2-GDNF treatment of alcohol versus an alternate reward: sucralose (cherry-flavored Splenda; 1.65% w/v). Briefly, 250 mL sucralose solution (probe) was accessible for 1 h to all the subjects followed by a 2-h period of only water. Probe sessions were run over 6 consecutive days during the second week of phase A4 and again during the second week of phase A6 ('SP1' and 'SP2' in Fig. 1a, respectively) per a modified induction program (as above), but with only a single food pellet delivered to signal the session start. These probe sessions were run during the timeout period between the regularly scheduled 21-h drinking sessions.

Post-mortem tissue collection and processing

Subjects were humanely euthanized with ketamine (10 mg kg^{-1}) and maintained on isoflurane during the craniotomy procedure that

optimizes the brain for subsequent electrophysiological procedures²⁷. Each brain was hemisected in situ, and the left hemisphere was removed without perfusion. The right carotid artery was cannulated, and the right hemisphere was perfused with oxygen-saturated artificial cerebrospinal fluid (aCSF) and then collected. Hemispheres were cut into 3-mm coronal blocks using a customized brain matrix (Electron Microscopy Sciences, Hatfield, PA). The ventral striatum (including NAc) and the midbrain (including VTA and substantia nigra) were dissected from the relevant right hemisphere blocks for voltammetry and electrophysiology. All remaining right hemisphere blocks, and blocks remaining after slices were taken for voltammetry, were post-fixed by immersion in 4% paraformaldehyde overnight and then transferred to 30% sucrose for future analyses. All left hemisphere blocks were snap-frozen on dry ice for subsequent use in GDNF ELISA and HPLC analyses.

Immunohistochemistry

A sliding freezing microtome was used to cut 40- μ m serial sections for histological processing. Free-floating tissue was then used for immunohistochemical staining⁷⁴. Free-floating sections were processed in 1% H₂O₂ for 20 min, washed in PBS with 0.1% Tween-20, blocked in animal-free buffer (Vector, SP5030) and incubated for 24 h with either 1:1,000 mouse-anti-TH (Millipore, MAB318), 1:1,000 monoclonal rabbit anti-GFP (Molecular Probes, G10362), or goat-anti-GDNF (R&D Systems, AF-212-NA). Probed tissue was then incubated for 1 h with horse anti-mouse HRP (Vector, MP-7402) or goat-on-rodent HRP Polymer (Biocare, GHP516), respectively. Stains were developed using Vector DAB Substrate Kit (SK-4100) with (for GDNF) or without (for TH) nickel. Tissue was mounted on slides and coverslipped with permanent media, and images were acquired using a Zeiss AxioScan microscope at $\times 20$ magnification using ZEN Blue software.

GDNF ELISA

The tissue concentration of GDNF was determined from VTA tissue punches with a commercially available human GDNF ELISA kit (Bio-Techne R&D Systems, DY212). ELISA was performed according to the manufacturer's protocol except for color development and absorbance reading, which was replaced with a chemiluminescent substrate kit (SuperSignal ELISA pico chemiluminescent substrate, Thermo Scientific). Total protein concentration was determined with a DC protein assay kit (Bio-Rad) according to the manufacturer's protocol.

HPLC analysis

Tissue punches from the VTA, NAc, substantia nigra, ventral putamen, caudate nucleus, cingulate gyrus and prefrontal cortex were homogenized by sonication in 250 μ l of 0.4 M perchloric acid and then centrifuged for 15 min at 10,000 $\times g$. The supernatants were filtered and the concentration of DA, homovanillic acid (HVA), 3,4-dihydroxyphenylacetic acid (DOPAC), 5-hydroxytryptamine (5HT) and 5-hydroxyindoleacetic acid (5-HIAA) was determined by HPLC using an ESA CoulArray 5600A HPLC system coupled to an electrochemical detector (HPLC-ECD)³⁸. All standards were purchased from Millipore-Sigma (-DOPA: cat. D-9628; DA: cat. H8502; DOPAC: cat. 850217; HVA: cat. H1252; 5-HT: cat. H9523; 5-HIAA: cat. H8876). Supernatant (30 μ l) was injected onto the HPLC-ECD system via autosampler and separated on a reverse-phase, analytical column MD-150X3.2 (DIONEX; cat. 70-0636) with a mobile MD-TM phase (DIONEX; cat. 70-1332) and flow rate of 0.5 ml min⁻¹. A series of monoamine standard solutions with known values (1,000 ng ml⁻¹, 100 ng ml⁻¹ and 20 ng ml⁻¹) were run in parallel. ECD peaks of monoamines in the samples were identified by peak retention times of the known standards. Areas under the ECD peaks for standards and samples were quantified using CoulArray Data Station 3.00 software. The amount of total protein was determined in the pellet fractions after

resuspension in 0.5 M NaOH with a DC protein assay kit (Bio-Rad, cat. 5000111) and Perkin Elmer Bio Assay Reader. Values were expressed as picomoles per milligram protein.

Ex vivo fast-scan cyclic voltammetry

Acute slices containing the NAc (250- μ m thick) were prepared with a vibrating microtome equipped with a ceramic blade and then placed into a holding chamber of oxygenated aCSF at room temperature (containing NaCl 126 mM, KCl 2.5 mM, NaH₂PO₄ 1.2 mM, CaCl₂ 2.4 mM, MgCl₂ 1.2 mM, NaHCO₃ 25 mM, ascorbic acid 0.4 mM, D-glucose 11 mM, pH 7.4). Slices were transferred to a recording chamber containing oxygenated aCSF (32 °C) and held in position with 0.5-cm platinum bars. DA was measured by applying a triangular waveform (-0.4 to +1.2 to -0.4 V vs Ag/AgCl at 400 V/s, every 100 ms) to a carbon fiber microelectrode (CFE, -150–200 μ m length, 7 μ m diameter). DA release was evoked by either single-pulse stimulation (750 μ A, 4 ms, monophasic) applied every 3 min, or by trains of stimulation (multipulse; 10 pulses, 750 μ A, 4 ms, monophasic, at 10, 20, 40 or 60 Hz) applied every 5 min through a bipolar stimulating electrode placed approximately 100 μ m from the CFE on the surface of the slice in the NAc. Stimulations continued until the peak height of evoked DA release was stable (three collections in a row with $\leq 10\%$ variability) to ascertain basal DA kinetics. Following acquisition of a stable baseline, alcohol (22 mM, 44 mM), quinpirole (30 nM, 100 nM), U50,488 (0.3 μ M, 1 μ M), or DH β E (100 nM) was applied to separate slices.

In addition to the eight male macaques used in this study, data were collected from recordings as above on a cohort of four ethanol- and experimentally-naïve adult male rhesus macaques (*Macaca mullatta*; 4.0–5.5 years at assignment; ONPRC breeding facility) and are represented as naïve control in Fig. 6a–c. These males comprised a co-housed control cohort in a separate study design that only contained experimental subjects, as described previously⁷⁵.

Statistical analyses

Before applying statistical approaches that assume Gaussian (normal) distributions, each data set was first evaluated by the Shapiro-Wilk test to assess normality. For multiple comparisons, either one- or two-way ANOVA with Geisser-Greenhouse correction was conducted, followed by the Holm-Sidak post-hoc test for pairwise comparisons when appropriate. A generalized linear mixed-effects model was used if randomly missing values were present. When comparing only two groups, a two-tailed Student's *t*-test for parametric distributions was used. A simple linear regression was used to determine the relationship between BECs and grams per kilogram alcohol intakes. *P* values ≤ 0.05 were considered significant. The statistical tests and group sizes (*n*) used for each analysis are noted in the respective figure legend. Prism software (GraphPad Software) was used for all statistical analyses and graphing.

Reporting summary

Further information on research design is available in the Nature Portfolio Reporting Summary linked to this article.

Data availability

The data that support the findings of this study, including behavioral, biochemical, and voltammetry analyses, are available on the public data repository Zenodo.org at <https://zenodo.org/record/7236274>.

References

- Helms, C. M. et al. The effects of age at the onset of drinking to intoxication and chronic ethanol self-administration in male rhesus macaques. *Psychopharmacology* **231**, 1853–1861 (2014).
- Green, K. L. et al. Comparison of ethanol metabolism in male and female cynomolgus macaques (*Macaca fascicularis*). *Alcohol Clin. Exp. Res.* **23**, 611–616 (1999).

63. Welsh, J. P. et al. Bidirectional plasticity in the primate inferior olive induced by chronic ethanol intoxication and sustained abstinence. *Proc. Natl Acad. Sci. USA* **108**, 10314–10319 (2011).
64. Kells, A. P. et al. Regeneration of the MPTP-lesioned dopaminergic system after convection-enhanced delivery of AAV2-GDNF. *J. Neurosci.* **30**, 9567–9577 (2010).
65. Su, X. et al. Real-time MR imaging with gadoteridol predicts distribution of transgenes after convection-enhanced delivery of AAV2 vectors. *Mol. Ther.* **18**, 1490–1495 (2010).
66. Breese, G. R., Sinha, R. & Heilig, M. Chronic alcohol neuroadaptation and stress contribute to susceptibility for alcohol craving and relapse. *Pharmacol. Ther.* **129**, 149–171 (2011).
67. Koob, G. F. Alcoholism: allostasis and beyond. *Alcohol Clin. Exp. Res.* **27**, 232–243 (2003).
68. Rodd, Z. A. et al. Effects of repeated alcohol deprivations on operant ethanol self-administration by alcohol-preferring (P) rats. *Neuropsychopharmacology* **28**, 1614–1621 (2003).
69. Lopez, M. F. & Becker, H. C. Effect of pattern and number of chronic ethanol exposures on subsequent voluntary ethanol intake in C57BL/6J mice. *Psychopharmacology* **181**, 688–696 (2005).
70. Baker, E. J., Farro, J., Gonzales, S., Helms, C. & Grant, K. A. Chronic alcohol self-administration in monkeys shows long-term quantity/frequency categorical stability. *Alcohol Clin. Exp. Res.* **38**, 2835–2843 (2014).
71. Ford, M. M., Steele, A. M., McCracken, A. D., Finn, D. A. & Grant, K. A. The relationship between adjunctive drinking, blood ethanol concentration and plasma corticosterone across fixed-time intervals of food delivery in two inbred mouse strains. *Psychoneuroendocrinology* **38**, 2598–2610 (2013).
72. Witkiewitz, K. & Tucker, J. A. Abstinence not required: Expanding the definition of recovery from alcohol use disorder. *Alcohol Clin. Exp. Res.* **44**, 36–40 (2020).
73. Shabani, S. et al. A genetic animal model of differential sensitivity to methamphetamine reinforcement. *Neuropharmacology* **62**, 2169–2177 (2012).
74. Naidoo, J. et al. Extensive transduction and enhanced spread of a modified AAV2 capsid in the non-human primate CNS. *Mol. Ther.* **26**, 2418–2430 (2018).
75. Jimenez, V. A. et al. Synaptic adaptations in the central amygdala and hypothalamic paraventricular nucleus associated with protracted ethanol abstinence in male rhesus monkeys. *Neuropsychopharmacology* **44**, 982–993 (2019).

Acknowledgements

We thank N. Newman, K. Diem, H. Vander Jagt, C. Rudnicky, J. Schoen and J. Mootz for animal husbandry and data collection of daily drinking sessions; S. Gonzales for technical support with drinking session programming and equipment maintenance; and B. Park for consultation with statistical modeling and experimental design. We also acknowledge the contributions of C. Kroenke and M. Reusz for MRI support; L. Martin and T. Hobbs for surgical services support; A. Lewis, A. Johnson and L. Colgin, as well as W. Price and A. Beckman, for pathology services support; M. Travis and V. Sudhakar for histology support; the Electrophysiology Core overseen by V. Cuzon-Carlson for hosting and supporting the voltammetry experiments; the Molecular Virology Core at the Oregon National Primate Research Center (ONPRC) for performing viral serology assays; and the Clinical Pathology Laboratory (ONPRC) for conducting in-house assays for complete blood count and a comprehensive chemistry panel.

This study was funded by National Institute on Alcohol Abuse and Alcoholism (NIAAA) grant R01 AA024757 (to M.M.F.). Additional support was provided by NIH grants U01 AA013510 (K.A.G.), U01 AA014091 (S.R.J.), P60 AA010760 (K.A.G. and M.M.F.), R24 AA019431 (K.A.G.) and P50 AA026117 (S.R.J.).

Author contributions

M.F. supervised the research and oversaw coordination across laboratories, designed and performed experiments, analyzed and interpreted data and wrote and edited the manuscript. B.G. and K.H. performed voltammetry experiments, analyzed and interpreted data, assisted in drafting results section and edited the manuscript. V.V. performed tissue immunohistochemistry and microscopy, assisted on data analysis and interpretation, and assisted with manuscript writing and editing. J.N. assisted with coordination of intra-VTA infusions, analyzed GDNF ELISA and HPLC results, and assisted in drafting the results section. P.H. performed ELISA experiments, assisted with interpretation of viral serology results, and edited the manuscript. L.V. served as project lead of animal cohort, collected and analyzed data, coordinated institutional services associated with husbandry, surgery, MRI, and pathology, and edited the manuscript. E.P. and M.D. performed voltammetry experiments on housing control NHPs and assisted in collecting and interpreting voltammetry data. K.O. performed HPLC experiments and assisted with interpretation of HPLC results. J.B. assisted with surgeries and consulted on tissue collection and handling techniques. L.S. consulted on tissue collection and handling techniques and assisted with manuscript writing and editing. J.M. performed brain tissue processing and edited the manuscript. J.F. participated in project inception, and assisted with manuscript writing and editing. S.J. designed voltammetry experiments, interpreted data, supervised B.G., K.H., E.P., and M.D., and edited the manuscript. K.G. and K.B. conceived the project, provided feedback on data analyses, and edited the manuscript. K.G. supervised M.F. and L.V. whereas K.B. supervised J.N., P.H., J.B., L.S., V.V. and J.F. on their efforts. K.B. performed the MRI-guided infusions targeting the VTA.

Competing interests

K.S.B. is a consultant for Asklepios BioPharmaceutical, Scribe Therapeutics and Aviado Bio. The remaining authors declare no competing interests.

Additional information

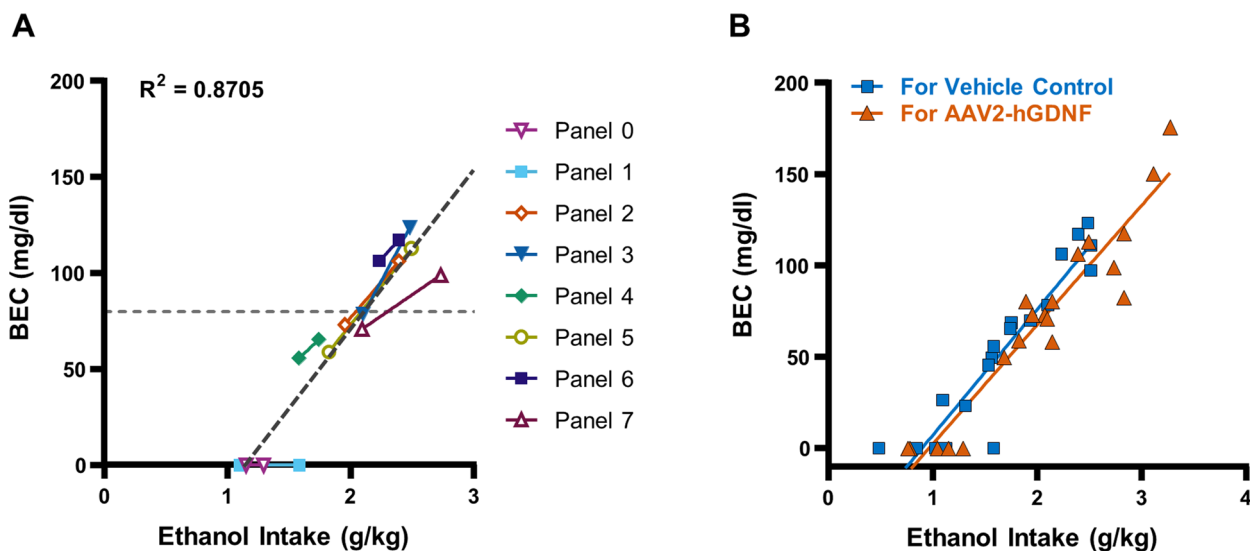
Extended data is available for this paper at <https://doi.org/10.1038/s41591-023-02463-9>.

Supplementary information The online version contains supplementary material available at <https://doi.org/10.1038/s41591-023-02463-9>.

Correspondence and requests for materials should be addressed to Kathleen A. Grant or Krystof S. Bankiewicz.

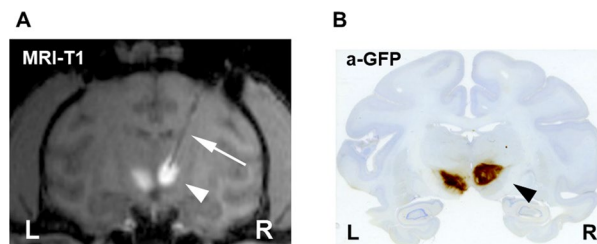
Peer review information *Nature Medicine* thanks Miguel Sena-Estevés, Alëna Balasanova and the other, anonymous, reviewer(s) for their contribution to the peer review of this work. Primary Handling Editor: Anna Maria Ranzoni, in collaboration with the *Nature Medicine* team.

Reprints and permissions information is available at www.nature.com/reprints.



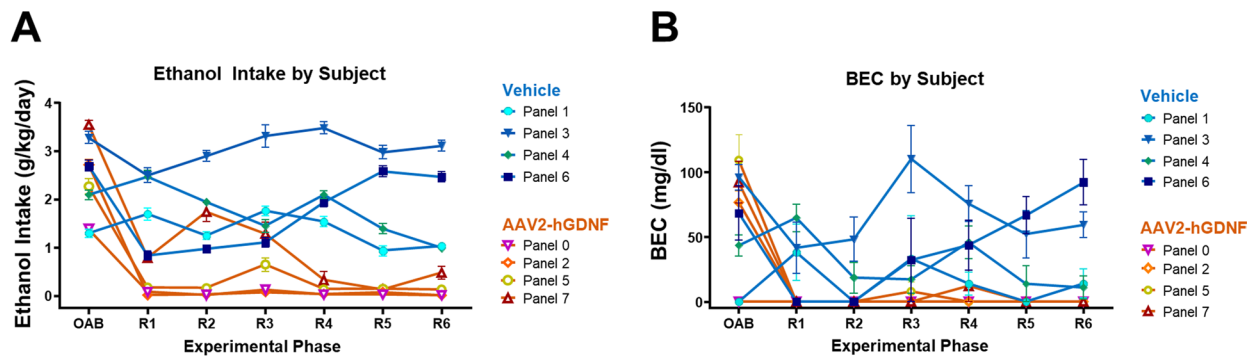
Extended Data Fig. 1 | Chronic alcohol self-administration in rhesus macaques. a) The relationship between blood ethanol concentrations (BECs) collected during the final week of the OAB ($n = 2$ per subject) and corresponding alcohol intakes recorded at timing of sampling for each subject as identified by drinking panel each was assigned (Panel 0–7), with the dashed horizontal line demarcating 80 mg/dl (the threshold for legal intoxication in humans). 6 of the 8 subjects exhibited alcohol consumption approaching or surpassing the 80 mg/dl

threshold during the final week of OAB. **b)** The relationship between BECs collected during the final two months of the OAB and corresponding alcohol intakes recorded at timing of sampling divided between subjects destined for the Vehicle-treated control group and the AAV2-hGDNF-treated group (4 subjects per group, $n = 20$ BEC points per group), demonstrating the similarity of BEC-alcohol intake relationship between the two groups.



Extended Data Fig. 2 | Pilot surgeries for AAV2 delivery to the VTA. Prior to viral drug infusion of the experimental groups, a pilot study was conducted using two macaques to confirm surgical coordinates and trajectory planning, as well as infusate and transgene distribution within the VTA of macaques. AAV2-GFP spiked with gadolinium chelate (2 mM, ProHance, Bracco Diagnostics, Princeton, NJ, USA) was bilaterally infused into the VTA target via magnetic-resonance imaging-guided convection-enhanced delivery (MR-guided CED) followed by post-mortem immunohistochemical assessment of GFP protein expression. Below are representative images of MRI with gadoteridol contrast (**a**) and post-mortem immunohistochemical staining

for GFP (**b**) from one of two preliminary macaque subjects used to confirm targeting and vector distribution in the VTA. AAV2 vector encoding green fluorescent protein (GFP) was delivered by CED as described in Methods. The white arrow (**A**) shows the cannula actively delivering the vector with contrast agent and the white arrowhead (**A**) shows the imaging detection of the contrast in the infusate. One month following infusion, subjects were sacrificed by intracardial perfusion, and brain tissue harvested for immunochemical analyses to address GFP expression and distribution (**B**). The black arrowhead (**B**) shows the positive immunochemical staining for the GFP antibody.

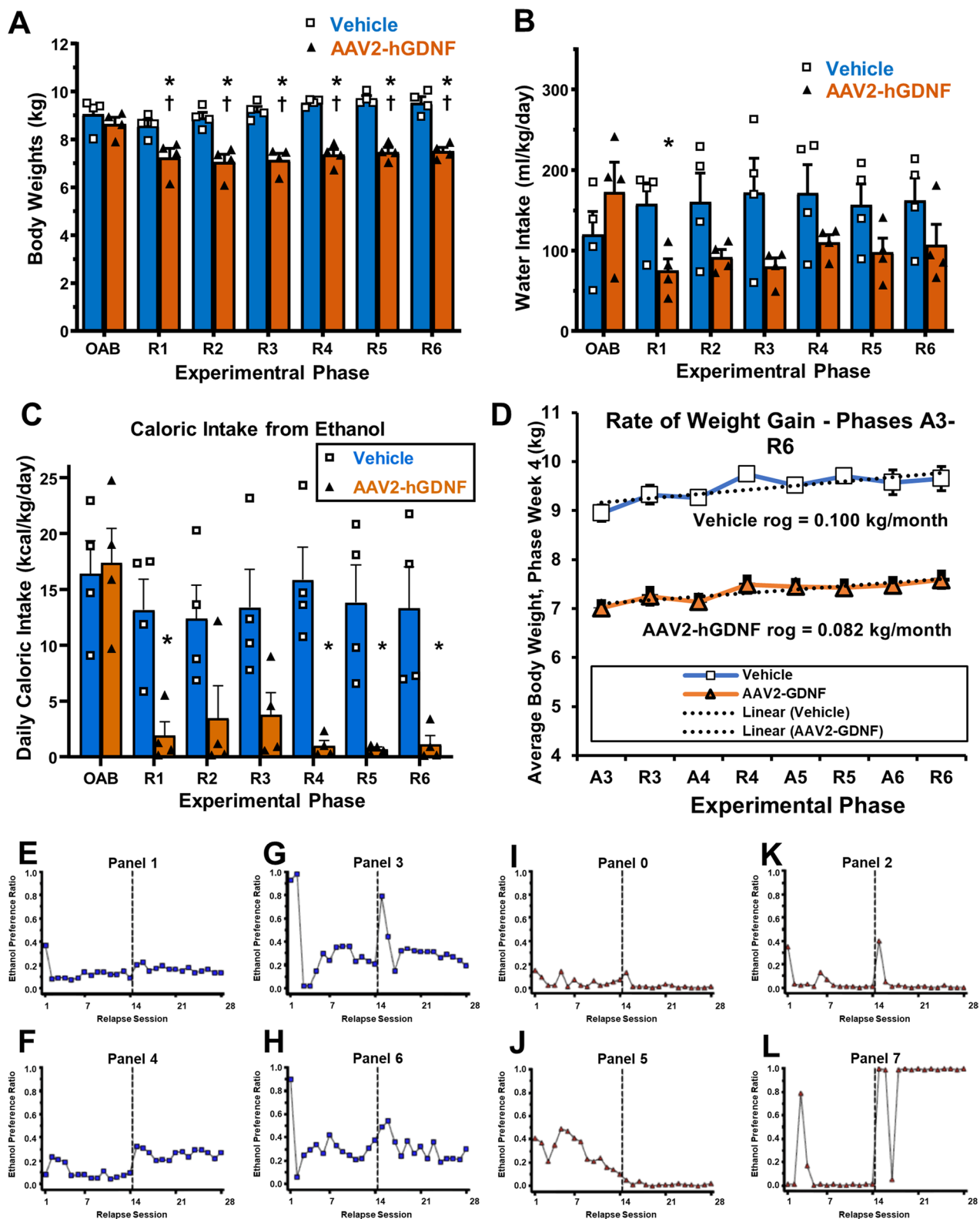


C Ethanol drinking patterns during each alcohol reintroduction onset (day 1) as a factor of AAV2-hGDNF treatment.

	Experimental Phase						
	OAB	R1	R2	R3	R4	R5	R6
Ethanol Intake^{†, ‡}							
Vehicle	2.47 ± 0.40	3.27 ± 0.51	2.51 ± 0.35	3.04 ± 0.84	2.95 ± 0.40	2.70 ± 0.46	2.43 ± 0.64
AAV2-GDNF	2.51 ± 0.49	0.52 ± 0.45 ^{***#}	0.64 ± 0.47 ^{**#}	0.76 ± 0.40 [#]	1.11 ± 0.99	0.09 ± 0.04 ^{*##}	0.17 ± 0.07 ^{*#}
Bout Frequency[†]							
Vehicle	18.3 ± 5.4	20.3 ± 4.6	14.8 ± 0.8	13.0 ± 0.9	17.8 ± 1.8	16.8 ± 2.4	16.8 ± 4.2
AAV2-GDNF	12.4 ± 1.8	6.8 ± 4.2	7.5 ± 3.0	12.3 ± 5.2	7.3 ± 4.7	2.8 ± 0.8	3.3 ± 1.9
Median Bout Size							
Vehicle	25.9 ± 7.1	28.1 ± 12.6	27.1 ± 7.6	28.4 ± 11.3	20.1 ± 6.7	16.6 ± 3.4	17.3 ± 6.2
AAV2-GDNF	38.8 ± 12.9	4.6 ± 2.9	8.8 ± 3.1	8.0 ± 3.6	11.0 ± 8.8	5.6 ± 2.3	12.4 ± 5.3
Latency to 1st Bout[†]							
Vehicle	10.2 ± 4.8	0.7 ± 0.3	4.7 ± 2.1	2.1 ± 1.9	2.9 ± 0.9	3.6 ± 0.8	2.5 ± 1.4
AAV2-GDNF	21.8 ± 9.5	1.1 ± 0.4	19.1 ± 12.5	14.7 ± 6.3	8.5 ± 3.6	19.2 ± 5.1	13.8 ± 5.6
1st Bout Size[†]							
Vehicle	63.7 ± 22.8	73.0 ± 52.5	90.7 ± 52.0	132.7 ± 73.5	89.1 ± 28.9	231.3 ± 18.9	55.7 ± 44.9
AAV2-GDNF	62.1 ± 13.3	5.6 ± 3.7	8.6 ± 4.5	13.2 ± 6.0	16.2 ± 15.4	4.8 ± 2.2	7.8 ± 6.2
Latency to Max Bout[†]							
Vehicle	129.2 ± 64.0	83.6 ± 36.7	147.8 ± 91.6	112.6 ± 53.2	160.8 ± 103.7	35.8 ± 8.1	110.8 ± 60.6
AAV2-GDNF	225.6 ± 56.9	175.6 ± 72.3	387.7 ± 142.4	518.3 ± 105.5	323.0 ± 107.2	251.6 ± 73.5	337.8 ± 97.8
Max Bout Size^{†, ‡}							
Vehicle	128.5 ± 19.2	156.9 ± 31.8	157.5 ± 19.6	166.2 ± 65.4	158.8 ± 23.2	231.3 ± 18.9 ^{***}	220.2 ± 34.4 [*]
AAV2-GDNF	121.3 ± 18.4	21.1 ± 13.8 ^{###}	41.3 ± 26.1 ^{*#}	31.8 ± 18.1 [*]	31.2 ± 19.7 ^{###}	8.7 ± 4.0 ^{***##}	17.1 ± 5.9 ^{###}

Extended Data Fig. 3 | Individual Monthly Ethanol intakes and BECs, and Table of Day 1 Reintroduction Statistics. a) Monthly individual subject means of daily alcohol intakes (g/kg/day) across each of the six alcohol reintroduction periods (R1–R6). b) Monthly individual subject means of BECs (mg/dl) across all six alcohol reintroduction periods (R1–R6). c) Table values and statistics of ethanol drinking patterns during each alcohol reintroduction onset (day 1) as a factor of AAV2-hGDNF treatment. All values represent the mean ± SEM of each treatment (n = 4/group). OAB measures reflect the grand mean from the final

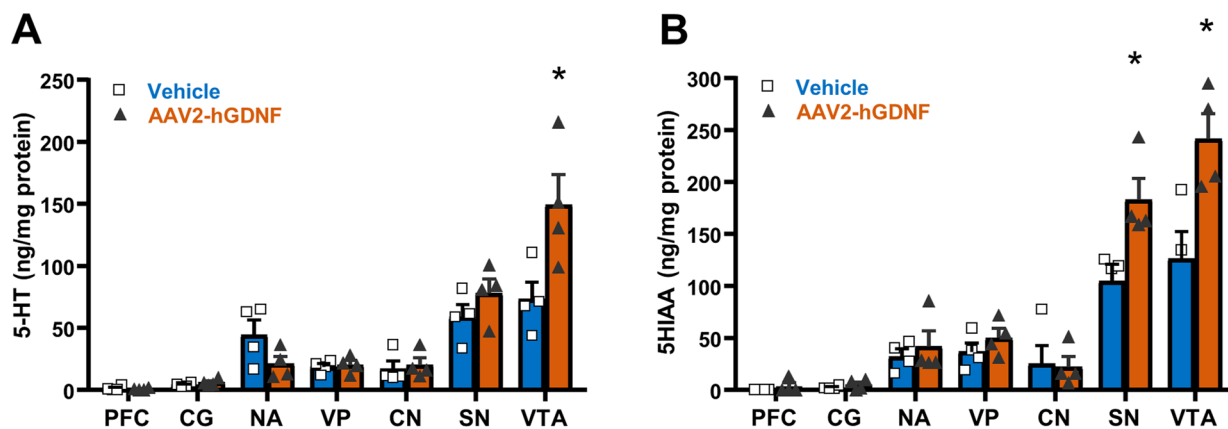
7 days of access to ethanol prior to the first forced abstinence (A1) phase onset while measures for alcohol reintroduction phases (R1–R6) are representative of the initial day of alcohol reintroduction following abstinence. †Significant main effects of AAV2-hGDNF treatment; ‡significant treatment x phase interactions. (Mean ± SEM; n = 4/group are shown; *; p ≤ 0.05 and **; p ≤ 0.001 vs. respective Vehicle-treated control group value. Specific statistical tests and p-values are as provided in Fig. 3).



Extended Data Fig. 4 | See next page for caption.

Extended Data Fig. 4 | Effects of AAV2-hGDNF on food and water intake, weight, and sensorimotor tasks in macaques. a) Monthly averages of subject weight (kg) shown by group (AAV2-hGDNF in orange; Vehicle in blue) from the last month of OAB and during alcohol reintroduction phases R1 through R6 (Mean \pm SEM; $n = 4$ /group; †: significant from within-group OAB value; *: significant from respective Vehicle group in phase [pairwise comparison using Students two-sided T-test]; R1 †, $p = 0.0230$, *, $p = 0.0231$; R2 †, $p = 0.00938$, *, $p = 0.00334$; R3 †, $p = 0.00703$, *, $p = 0.00066$; R4 †, $p = 0.0103$, *, $p = 0.000103$; R5 †, $p = 0.0109$, *, $p = 0.00005$; and R6 †, $p = 0.0103$, *, $p = 0.000369$). **b)** Monthly averages of subject water intake (ml/kg/day) shown by group (AAV2-hGDNF in orange; Vehicle in blue) from the last month of OAB and during alcohol reintroduction phases R1 through R6 (mean \pm s.e.m.; $n = 4$ /group; *: significant from respective Vehicle group in phase [pairwise comparison using Students two-sided T-test]; R2 *, $p = 0.0303$). **c)** The average daily caloric intake (kcal/kg/day) from ethanol (7 kcal/g) during the reintroduction phases for the Vehicle-treated (blue) and the AAV2-hGDNF-treated (orange) macaque groups (Mean \pm SEM; $n = 4$ /group; *: significant from respective Vehicle group in phase [pairwise comparison using Students two-sided T-test]; R1 *, $p = 0.00968$; R4 *, $p = 0.00249$; R5 *, $p = 0.00806$; and R6 *, $p = 0.0182$). **d)** The average group body weight in the final week of each phase in Phases A3-R6 for the Vehicle-treated and

AAV2-hGDNF-treated groups. Linear regression lines represent the calculated rate-of-gain during this 8mo time period (0.100 kg/mo for Vehicle, 0.082 kg/mo for AAV2-hGDNF; (Mean \pm SEM; $n = 4$ /group). **E-L)** Panel Reversal Test in R3. Starting on day 12 of experimental phase R2, one GDNF-treated subject (panel 7) inexplicably developed an absolute side preference for the spout designated for alcohol access that was unrelated to any malfunction in apparatus. During the first week of phase R2 this subject consumed 0.94 g/kg/day of alcohol and exhibited an alcohol preference ratio (a measure of choosing alcohol versus water intake) of 0.13, but by the final week of phase R2 this drinking profile switched to 2.71 g/kg/day and a ratio of 0.98. To determine whether this shift in behavior was due to a side bias versus a change in motivation to consume alcohol, the spout designated for alcohol delivery for all subjects was reversed for the first 2 weeks of phase R3 and then returned to original position for the second 2 weeks of this alcohol reintroduction period (see 'R' in Fig. 1a). This evaluation clearly demonstrated that each subject, with the exception of the GDNF-treated subject on panel 7 (L), could track the location of the alcohol spout while maintaining a comparable preference ratio. Starting with phase R4, the alcohol spout for GDNF-treated subject on panel 7 was kept in the reversed position so that the subject had daily access to water and could still access ethanol for evaluation.



C

	Brain Region						
	PFC	CG	NAc	VP	CN	SN	VTA
GDNF Protein (ng/mg total protein)							
Vehicle	0.045 ± 0.0065	0.043 ± 0.0095	0.120 ± 0.0204	0.053 ± 0.0048	0.063 ± 0.0125	--	--
AAV2-hGDNF	0.410 ± 0.0682**	1.063 ± 0.1524**	47.73 ± 12.48**	38.41 ± 12.08*	19.10 ± 6.664*	--	--
Dopamine (ng/mg total protein)							
Vehicle	6.3 ± 0.2	8.3 ± 3.4	757.9 ± 91.9	1211.7 ± 177.0	1155.5 ± 239.9	384.0 ± 93.9	222.3 ± 17.0
AAV2-hGDNF	5.4 ± 0.7	8.0 ± 0.6	1362.7 ± 351.1	1534.4 ± 153.0	1871.2 ± 288.0	611.2 ± 84.2	1290.5 ± 177.1**
DOPAC (ng/mg total protein)							
Vehicle	1.3 ± 0.8	5.6 ± 1.7	208.2 ± 26.2	301.3 ± 86.0	125 ± 16.3	75.5 ± 12.8	76.3 ± 11.3
AAV2-hGDNF	0.8 ± 0.5	5.8 ± 0.5	627.4 ± 142.3*	531.8 ± 183.6	226.0 ± 51.3	194.0 ± 21.8*	597.9 ± 53.5**
HVA (ng/mg total protein)							
Vehicle	11.9 ± 5.3	34.8 ± 5.1	903.6 ± 159.5	1373.3 ± 198.5	574.0 ± 26.1	509.8 ± 107.6	483.2 ± 61.7
AAV2-hGDNF	19.3 ± 3.7	101.5 ± 13.8*	2603.4 ± 438.9*	3371.2 ± 475.6*	2124.3 ± 419.0*	1106.6 ± 98.2*	1443.5 ± 171.6*
5HT (ng/mg total protein)							
Vehicle	1.2 ± 1.0	4.0 ± 0.8	44.7 ± 11.6	18.8 ± 2.5	17.2 ± 6.4	58.9 ± 9.9	73.2 ± 13.9
AAV2-hGDNF	0.75 ± 0.5	6.1 ± 1.4	21.3 ± 6.0	20.4 ± 3.4	20.5 ± 5.6	78.3 ± 11.3	149.3 ± 24.7*
5HIAA (ng/mg total protein)							
Vehicle	0 ± 0	2.1 ± 0.8	32.4 ± 6.8	36.8 ± 8.5	25.5 ± 17.4	104.6 ± 15.9	126.6 ± 26.1
AAV2-hGDNF	3.4 ± 3.4	5.1 ± 2.4	42.0 ± 14.7	50.4 ± 8.6	22.5 ± 9.8	183.1 ± 20.0*	241.6 ± 24.3*

Extended Data Fig. 5 | AAV2-hGDNF effects on 5HT concentrations and metabolism. **a**) Concentrations of 5HT (VTA: **, $p = 0.0359$ vs. respective Vehicle-treated control group value via two-tailed Student's T-test), and **(b)** its metabolite 5HIAA (SN: *, $p = 0.0220$; VTA: *, $p = 0.0179$ vs. respective Vehicle-treated control group value via two-tailed Student's T-test) in ng/mg protein as determined by HPLC from tissue homogenates. **c**) Table of values detected for GDNF protein

via ELISA (ng/mg total protein) and monoamine amounts via HPLC (ng/mg total protein). These values were used to generate the graphs shown in Fig. 5 and Extended Fig. 5. (Mean ± SEM; $n = 4$ /group are shown; *: $p \leq 0.05$ and **: $p \leq 0.001$ vs. respective Vehicle-treated control group value. Specific statistical tests and p-values are as provided in Fig. 5 and above.).

Reporting Summary

Nature Portfolio wishes to improve the reproducibility of the work that we publish. This form provides structure for consistency and transparency in reporting. For further information on Nature Portfolio policies, see our [Editorial Policies](#) and the [Editorial Policy Checklist](#).

Statistics

For all statistical analyses, confirm that the following items are present in the figure legend, table legend, main text, or Methods section.

n/a Confirmed

- The exact sample size (n) for each experimental group/condition, given as a discrete number and unit of measurement
- A statement on whether measurements were taken from distinct samples or whether the same sample was measured repeatedly
- The statistical test(s) used AND whether they are one- or two-sided
Only common tests should be described solely by name; describe more complex techniques in the Methods section.
- A description of all covariates tested
- A description of any assumptions or corrections, such as tests of normality and adjustment for multiple comparisons
- A full description of the statistical parameters including central tendency (e.g. means) or other basic estimates (e.g. regression coefficient) AND variation (e.g. standard deviation) or associated estimates of uncertainty (e.g. confidence intervals)
- For null hypothesis testing, the test statistic (e.g. F , t , r) with confidence intervals, effect sizes, degrees of freedom and P value noted
Give P values as exact values whenever suitable.
- For Bayesian analysis, information on the choice of priors and Markov chain Monte Carlo settings
- For hierarchical and complex designs, identification of the appropriate level for tests and full reporting of outcomes
- Estimates of effect sizes (e.g. Cohen's d , Pearson's r), indicating how they were calculated

Our web collection on [statistics for biologists](#) contains articles on many of the points above.

Software and code

Policy information about [availability of computer code](#)

Data collection

Panel-recorded behavioral data: Food and fluid intake data were recorded using National Instruments LabView software Version 2011
 HPCL Data: Collected and analyzed using ESA CoulArray Software Version 3.05
 ELISA Data: Collected and analyzed using Bio Tek Microplate Reader and Imager Software Version Gen5
 Microscopy: Images obtained using Zeiss Zen Software Version 2.3 (blue edition)
 Voltammetry Data: Collected and analyzed using Demon Voltammetry and Analysis Software (<https://www.wakeforestinnovations.com/technologies/demon-voltammetry-and-analysis-software/>) .

All collected observational and analog data points were organized using Microsoft Excel spreadsheet software

Data analysis

HPCL Data: Collected and analyzed using ESA CoulArray Software Version 3.05
 ELISA Data: Collected and analyzed using Bio Tek Microplate Reader and Imager Software Version Gen5
 Voltammetry Data: Collected and analyzed using Demon Voltammetry and Analysis Software, written using National Instruments LabView software (<https://www.wakeforestinnovations.com/technologies/demon-voltammetry-and-analysis-software/>) .

All statistical analyses were completed using GraphPad PRISM software Versions 8 and 9

For manuscripts utilizing custom algorithms or software that are central to the research but not yet described in published literature, software must be made available to editors and reviewers. We strongly encourage code deposition in a community repository (e.g. GitHub). See the Nature Portfolio [guidelines for submitting code & software](#) for further information.

Data

Policy information about [availability of data](#)

All manuscripts must include a [data availability statement](#). This statement should provide the following information, where applicable:

- Accession codes, unique identifiers, or web links for publicly available datasets
- A description of any restrictions on data availability
- For clinical datasets or third party data, please ensure that the statement adheres to our [policy](#)

Data sets generated for this study, including behavioral, biochemical, and voltammetry analyses, are available on the public data repository Zenodo.org at <https://zenodo.org/record/7236274>.

Human research participants

Policy information about [studies involving human research participants and Sex and Gender in Research](#).

Reporting on sex and gender	The study did not involve human research participants
Population characteristics	The study did not involve human research participants
Recruitment	The study did not involve human research participants
Ethics oversight	The study did not involve human research participants

Note that full information on the approval of the study protocol must also be provided in the manuscript.

Field-specific reporting

Please select the one below that is the best fit for your research. If you are not sure, read the appropriate sections before making your selection.

Life sciences Behavioural & social sciences Ecological, evolutionary & environmental sciences

For a reference copy of the document with all sections, see nature.com/documents/nr-reporting-summary-flat.pdf

Life sciences study design

All studies must disclose on these points even when the disclosure is negative.

Sample size	Sample size: The sample size and power analyses were performed to detect a difference in alcohol intake (g/kg/day) between control and AAV2-GDNF treated groups of rhesus macaques based on status of pre-exposure to alcohol. A study of similar scope in rats reported mean \pm SEM alcohol intakes (g/kg/day) of 5.6 ± 0.44 and 2.9 ± 0.60 in rats infused intra-VTA with AAV2-GFP (control) or AAV2-GDNF, respectively, at 6 weeks post-treatment. The effect size of this rat study was 1.71. We predicted a similar result in our non-human primate model, and used the effect size from this earlier data to calculate sample size and power justification.
Data exclusions	No data were excluded
Replication	The experimental design was focused on the between-group comparison between control and AAV2-GDNF treatment groups. However, dependent measures associated with alcohol drinking, food pellet consumption, water consumption and body weight (among others) were repeatedly assessed on a daily basis in order to establish the long-term trajectory and efficacy of the treatment. These repeated measures of key dependent variables allowed us to replicate our findings daily over an extended timeline of several months. Furthermore, we committed the animal groups to six cycles of abstinence-relapse in order to replicate the impact of AAV2-GDNF treatment over multiple, successive relapse opportunities. Similar approaches were taken with other behavioral measures associated with the raisin reach task, sucralose probe tests, etc. We found that all measures taken repeatedly replicated to express very similar impacts of AAV2-GDNF treatment.
Randomization	Experimental groups were counterbalanced for average g/kg alcohol intake during the final 4-weeks of open access phase 1. Since daily alcohol intake was our primary dependent measure of interest, we ensured that the two groups were matched by measure of central tendency (mean) as well as variability (standard error of the mean). To the extent possible, body weight, water intake, and blood ethanol concentrations achieved were taken into account during this counterbalancing process.
Blinding	Blinding was not observed in this study during behavioral assessments for multiple reasons. First, all investigators on the project were performing tasks at multiple levels (animal husbandry, data collection, data entry, and analysis) on a 7-day/week and 24-hr basis. This made it logistically difficult to uphold blinding. Second, the appearance of transient sensorimotor effects and modest body weight reductions in AAV2-GDNF treated animals required closer scrutiny by investigators and veterinary staff. Third, the behavioral data that was collected daily created obvious and stark differences between individual animals and their placement into the two groups. Biochemical samples for HPLC and ELISA analyses were deidentified and the experimenter blinded during sample processing and analyses.

Reporting for specific materials, systems and methods

We require information from authors about some types of materials, experimental systems and methods used in many studies. Here, indicate whether each material, system or method listed is relevant to your study. If you are not sure if a list item applies to your research, read the appropriate section before selecting a response.

Materials & experimental systems

n/a	Included in the study
<input type="checkbox"/>	<input checked="" type="checkbox"/> Antibodies
<input checked="" type="checkbox"/>	<input type="checkbox"/> Eukaryotic cell lines
<input checked="" type="checkbox"/>	<input type="checkbox"/> Palaeontology and archaeology
<input type="checkbox"/>	<input checked="" type="checkbox"/> Animals and other organisms
<input checked="" type="checkbox"/>	<input type="checkbox"/> Clinical data
<input checked="" type="checkbox"/>	<input type="checkbox"/> Dual use research of concern

Methods

n/a	Included in the study
<input checked="" type="checkbox"/>	<input type="checkbox"/> ChIP-seq
<input checked="" type="checkbox"/>	<input type="checkbox"/> Flow cytometry
<input type="checkbox"/>	<input checked="" type="checkbox"/> MRI-based neuroimaging

Antibodies

Antibodies used

Goat-anti-GDNF, R&D Systems, catalog number: AF-212-NA, at 1:1000 dilution
 Mouse-anti-TH, Millipore, catalog number: MAB318, clone LNC1, at 1:1000 dilution
 Rabbit anti-GFP, Molecular Probes, catalog number: G10362, at 1:1,000

Validation

The goat-anti-GDNF from R&D Systems is a polyclonal antibody reported in their documentation of the product to detect rat and human GDNF. The immunogen used to generate the antibody was a A109-I211 human GDNF peptide. We have previously reported using this antibody to detect virus-mediated human GDNF expression in non-human primate brain: Gimenez et al., Neuroimage, 54: S189-S195, 2011.

The mouse-anti-TH antibody from Millipore is a monoclonal antibody derived from the hybridoma clone LNC1. This antibody is reported by Millipore and others to have broad species reactivity to tyrosine hydroxylase, including monkey, and has been widely used and published, including previously by our group in monkey: Green F, Samaranch L, Zhang HS, Manning-Bog A, Meyer K, Forsayeth J, Bankiewicz KS. Axonal transport of AAV9 in nonhuman primate brain. Gene Ther. 2016 Jun;23(6):520-6. doi: 10.1038/gt.2016.24. Epub 2016 Mar 8. PMID: 26953486; PMCID: PMC4893316.

The rabbit-anti-GFP from Molecular Probes is a recombinant monoclonal (unknown clone) antibody raised against full-length GFP as an antigen. This antibody is reported by Molecular Probes and others to have high specificity to green fluorescent protein and has been widely used and published, including previously by our group in monkey: Samaranch L, Sebastian WS, Kells AP, Salegio EA, Heller G, Bringas JR, Pivrotto P, DeArmond S, Forsayeth J, Bankiewicz KS. AAV9-mediated expression of a non-self protein in nonhuman primate central nervous system triggers widespread neuroinflammation driven by antigen-presenting cell transduction. Mol Ther. 2014 Feb;22(2):329-337. doi: 10.1038/mt.2013.266. Epub 2013 Nov 21. PMID: 24419081; PMCID: PMC3918916.

Animals and other research organisms

Policy information about [studies involving animals](#); [ARRIVE guidelines](#) recommended for reporting animal research, and [Sex and Gender in Research](#)

Laboratory animals

rhesus macaque monkeys (n=14), 4.0 - 5.5 years of age

Wild animals

The study did not involve wild animals

Reporting on sex

Male rhesus macaques were used in this study. The vast majority of the historical data cited in support of the funded grant proposal was generated in male rhesus monkeys, and so it provided direct validation of our model and demonstrates the translational advantages of the current studies that were also run in male subjects. Given the apparent effectiveness of AAV2-GDNF treatment in males, it is warranted to run future studies including female macaques in the study design. Sex was assigned by primate veterinarians in sexually mature adults by visual inspection of external genitalia and secondary sex characteristics. Sex of each animal was further confirmed at autopsy.

Field-collected samples

The study did not involve field-collected samples

Ethics oversight

All procedures were performed in accordance with NIH guidelines on the care and use of laboratory subjects.
 All procedures were approved by the IACUC at the Oregon National Primate Research Center (ONPRC)

Note that full information on the approval of the study protocol must also be provided in the manuscript.

Experimental design

Design type	Resting State
Design specifications	Not Applicable: The MRI was utilized only to identify structures and guide the delivery of the drug based on previously reported methodology. These MRI images were interpreted in real time to assure proper placement of the delivery canulae. See "Infuse-as-you-go convective delivery to enhance coverage of elongated brain targets: technical note Vivek Sudhakar, Jerusha Naidoo, Lluís Samaranch, John R. Bringas, Russell R. Lonser, Massimo S. Fiandaca, and Krystof S. Bankiewicz, PhD019. pp. 530–537; vol. 133:2
Behavioral performance measures	Not Applicable: The behavioral performance measures obtained in this study were to determine differences between groups based on the drug delivered. All animals received an identical surgery.

Acquisition

Imaging type(s)	Structural
Field strength	3T
Sequence & imaging parameters	Three-dimensional, T1, magnetization-prepared, rapid gradient echo (3D-MPRAGE) images Repetition time (TR) = 2110 ms, echo time (TE) = 3.6 ms Flip angle = 15°, number of excitations (NEX) = 1 Matrix = 240 × 240, field of view (FOV) = 240 × 240 × 240 Slice thickness = 1 mm
Area of acquisition	3D-SPGR whole brain scan
Diffusion MRI	<input type="checkbox"/> Used <input checked="" type="checkbox"/> Not used

Preprocessing

Preprocessing software	Syngo MR B17
Normalization	No normalization required
Normalization template	Data not normalized
Noise and artifact removal	Not applicable, subject head was immobilized in stereotaxic frame
Volume censoring	Not applicable, no motion related artifacts were detected

Statistical modeling & inference

Model type and settings	Not applicable: The MRI was utilized only to identify structures and guide the delivery of the drug based on previously reported methodology. These MRI images were interpreted in real time to assure proper placement of the delivery canulae. See "Infuse-as-you-go convective delivery to enhance coverage of elongated brain targets: technical note Vivek Sudhakar, Jerusha Naidoo, Lluís Samaranch, John R. Bringas, Russell R. Lonser, Massimo S. Fiandaca, and Krystof S. Bankiewicz, PhD019. pp. 530–537; vol. 133:2
Effect(s) tested	Only for 3-D reconstruction
Specify type of analysis:	<input type="checkbox"/> Whole brain <input checked="" type="checkbox"/> ROI-based <input type="checkbox"/> Both
Anatomical location(s)	Ventral Tegmental Area
Statistic type for inference (See Eklund et al. 2016)	No statistical analysis was performed on the dicoms
Correction	Not applicable: The MRI was utilized only to identify structures and guide the delivery of the drug based on previously reported methodology. These MRI images were interpreted in real time to assure proper placement of the delivery canulae. See "Infuse-as-you-go convective delivery to enhance coverage of elongated brain targets: technical note Vivek Sudhakar, Jerusha Naidoo, Lluís Samaranch, John R. Bringas, Russell R. Lonser, Massimo S. Fiandaca, and Krystof S. Bankiewicz, PhD019. pp. 530–537; vol. 133:2

Models & analysis

- | n/a | Included in the study |
|-------------------------------------|---|
| <input checked="" type="checkbox"/> | <input type="checkbox"/> Functional and/or effective connectivity |
| <input checked="" type="checkbox"/> | <input type="checkbox"/> Graph analysis |
| <input checked="" type="checkbox"/> | <input type="checkbox"/> Multivariate modeling or predictive analysis |